ALMA MATER STUDIORUM
UNIVERSITÀ DI BOLOGNA

DEPARTMENT OF INDUSTRIAL CHEMISTRY "TOSO MONTANARI"

SECOND CYCLE DEGREE IN

LOW CARBON TECHNOLOGIES AND SUSTAINABLE CHEMISTRY

CLASSE LM-71 - SCIENZE E TECNOLOGIE DELLA CHIMICA INDUSTRIALE

Fire Behavior of Low Smoke Acidity PVC Compounds for Electrical Cables, I: Focus on Flammability and Smoke.

Supervisor

Prof. Laura Mazzocchetti

Co-Supervisor

Dr. Gianluca Sarti

Dr. Claudia Bandinelli

(Reagens S.p.A)

Dr. Emanuele Maccaferri

Candidate

Giuseppe Valvano

Session October 2024

Academic Year 2023/2024

Table of contents

ABSTRACT

Regulation (EU) No 305/2011 [1] lays down harmonized conditions for marketing construction products in the European Union (EU) such as cables permanently installed in buildings. One of the seven basic requirements of the CPR is safety in case of fire, and construction products must meet certain specific requirements in terms of reaction-to-fire. Tests, requirements, marking, controls, etc. on construction products must be the same in all EU countries, according to the product standard EN 50575 [2] which defines how cables are managed from their production to placing them on the market. On the other hand, the standard EN 13501-6 [3], provides the technical standards to be performed and the requirements to be met for specific reaction-to-fire classifications. In the dissertation several compounds PVC standard, PVC low smoke acidity and halogen free for Italian CPR cables were tested. The aim is verifying their fire performances at micro combustion calorimetry (MCC) and at Cone Calorimeter at different incidental heat fluxes (35 kW/m^2), near flash over conditions, and 62 kW/m^2 corresponding to a fully developed stage of a fire. The study's findings highlighted that in terms of flammability measured at MCC and THR at cone calorimetry all the new generation of low smoke acidity PVC compounds are better than the HF counterparts. The only exception is M16 jacket, which showed a better FIGRA justified by a higher TTP more than its pHRR. This last consideration demonstrates that M16 burns later but developing in the end the same heat release as R16 LSA. Thanks to this behavior, M16 is the key compound that protects the more flammable HF bedding and insulation, allowing FG16OM16 to meet the requested reaction-to-fire. In conclusion, the low smoke acidity PVC compounds grant a comparable flame retardancy and even the extremely low smoke production normally obtained with HFFR.

1. INTRODUCTION

1.1 PVC

Polyvinyl chloride (PVC) plays a crucial role in our everyday lives, accounting for 12.7% of the global plastic production by polymer. It ranks as the third most important plastic commodity, following polyethylene (PE) and polypropylene (PP) [4]. In PVC item production, additives are incorporated into the resin to facilitate its transformation into semi-finished compounds or fully realized articles. These additives serve multifaceted purposes, ranging from enhancing processability to imparting desired characteristics to the final product. The resultant articles can manifest as either rigid (PVC-U) or flexible (PVC-P) structures [40], catering to diverse applications across various sectors. In contemporary life, PVC is integral to numerous aspects of modern existence, making its presence known in residences, vehicles, workplaces, healthcare facilities, and beyond. From essential household items to specialized equipment, the versatility of PVC renders it indispensable across a multitude of industries and applications. The primary domain of PVC utilization is in the construction and building sector, where it is employed in many structural and decorative components. This encompasses electrical cables, window profiles, rolling shutters, gutters, rigid pipes and fittings, flooring, wall coverings, roofing membranes, and hoses, among other applications. The extensive use of PVC in construction highlights its reliability, durability, and adaptability to various environmental conditions. Beyond construction, PVC's versatility extends to several other sectors. In technical and food packaging, PVC functions as a reliable barrier material, protecting products and ensuring their integrity during storage and transportation, bringing strong support to sustainability. In the pharmaceutical industry, PVC plays a crucial role in the safe containment and delivery of medications, underscoring its importance in healthcare. Additionally, PVC's influence extends to the transportation sector, where it contributes to the fabrication of durable and lightweight components essential for vehicle construction. In the electronics and telecommunications fields, PVC supports technological advancements by enabling the seamless transmission of data and power. Even in fashion, PVC finds its niche, offering innovative solutions in textile manufacturing and design, from

protective clothing to stylish accessories, showcasing PVC's adaptability to the ever-evolving trends of the fashion industry [5].

Figure 1.1 provides a comprehensive overview of PVC resin consumption across various sectors in the European Union for the year 2022, underscoring the influence of PVC across diverse industries and applications.

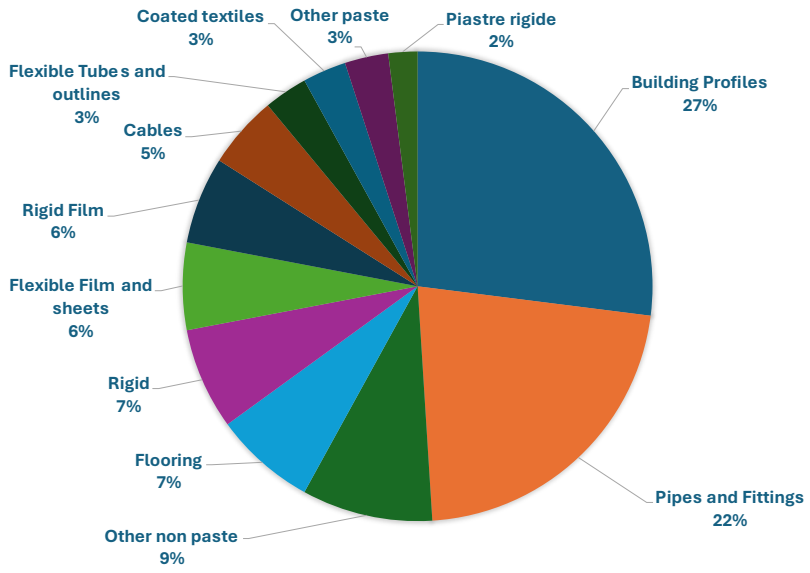

***Figure 1.1**: PVC resin consumption per article in the EU in 2022*

PVC compounds are essential in electrical cable production, where they are used as insulation, jacketing, and bedding materials. However, when subjected to combustion, PVC cable compounds release hydrogen chloride (HCl), generating acidic smoke. The concentration of HCl in the gas depends on the composition of additives within the PVC compounds, including fillers, plasticizers, flame retardants, and acid scavengers. As per standards outlined in EN 60754-1 [6], the concentration of HCl in PVC cable compounds can fluctuate significantly. Despite the initial release of HCl during combustion, it is noteworthy that gaseous HCl undergoes rapid decay within the surrounding environment. This decay process serves to diminish the overall

concentration of HCl present in the gas phase [7]. It is commonly acknowledged that the primary toxic component in the smoke remains carbon monoxide (CO).

Furthermore, the behavior of chemically reactive and highly hygroscopic species like hydrogen chloride introduces additional complexities. Chemical and physical reactions within the environment can significantly influence the airborne concentration of HCl. Studies, such as those conducted by Beitel et al., have explored real-world scenarios involving the decomposition of PVC cables due to electrical overload in confined spaces. Their findings revealed that only a fraction of the total chlorine available remains in the gas phase over time. For instance, after 45 minutes, approximately 3% of the initial chlorine persists in the gas phase, whereas other monitored gases, such as CO, exhibit no significant concentration decay [7].

While the development of acidity during cable combustion in fires can lead to respiratory tract irritation and potentially induce panic among affected individuals [8], the assessment of smoke acidity is not universally regarded as a primary life-saving measure within in fire science. Rather, experts emphasize the importance of evaluating a range of factors to gauge fire performance and assess the likelihood of uncontrolled fire propagation, notably beyond the critical threshold known as "flashover." Crucial among these factors is the measurement of heat released from burning materials, denoted as Total Heat Release (THR), along with the rate at which this heat is released, termed Heat Release Rate (HRR). Specifically, identifying the maximum peak of the heat release curve (pHRR) and assessing smoke density are deemed essential indicators [9,10,11]. The time to escape is furthermore affected by the smoke production from articles, which impede people to escape safely from fire scenario or to be rescued by fire fighters.

To mitigate heat release and smoke production, special additives called flame retardants and smoke suppressants are often incorporated into materials [12]. These additives play a crucial role in enabling a safe escape during fires, ensuring that people can escape unharmed before the onset of flashover without being hindered by dense smoke. Therefore, many countries prioritize these performance metrics over smoke acidity in their fire risk assessments, reflecting the prevailing consensus within the fire safety community.

1.2 PVC SYNTHESIS

PVC is a halogenated polymer having the structure in Figure 1.2:

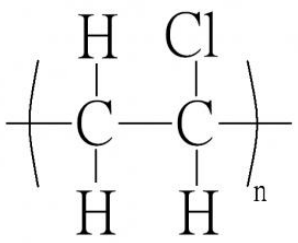

***Figure 1.2**: PVC structure.*

and its industrial production involves three different steps, to obtain in order, first chlorine, then the monomer and lastly the actual polymer.

Unlike other plastics, PVC relies predominantly on chlorine derived from table salt for its production. With a high chlorine content of nearly 60%, PVC inherently qualifies as a low carbon material. Chlorine industrial production is mainly carried out through a chloro-alkali electrochemical cell, which process aims at the synthesis of NaOH and Cl_2. Approximately 30% of all the worldwide Cl_2 produced by this process is used for the synthesis of PVC [13]. The concerted efforts towards developing new energy mixes across numerous European countries, coupled with the complete transition to the membrane electrolysis process, have yielded significant reductions in the environmental footprint associated with chlorine production in Europe over the past decade. According to the latest Environmental Product Declaration for chlorine, the Global Warming Potential impact witnessed a remarkable reduction of 22.3% from 2011 to 2020 [4]. These advancements have had a direct positive impact on the environmental footprint of PVC. Consequently, the environmental impacts associated with PVC production are automatically mitigated owing to these improvements in chlorine production processes.

There are two primary methods for producing vinyl chloride monomer (VCM): direct chlorination and oxychlorination. In the direct chlorination process, ethylene and chlorine react within a reactor containing a catalyst to form ethylene dichloride (EDC).

The EDC is then thermally cracked at a few hundred degrees Celsius to yield VCM. In the oxychlorination process, hydrogen chloride, produced as a by-product of the thermal cracking of EDC, reacts with ethylene in the presence of a catalyst and air (or oxygen), resulting in the formation of EDC. This EDC, after dehydration, is also thermally cracked to produce VCM. Major VCM plants in Western Europe typically combine these two methods to optimize production efficiency [14].

The third step is the radical polymerization of VCM. The product resulting from polyaddition ranges from 400 to 1000 monomer units, mostly arranged in an atactic structure and responsible for the amorphous structure of PVC. The synthesis of PVC involves a polyaddition reaction between the monomers, which can be carried out using different polymerization techniques [13]:

- Bulk polymerization, does not use solvents, suspending agents or emulsifiers but only involves the use of the monomer which, as the reaction proceeds, forms the insoluble polymer in the monomer that has not reacted yet. Given the type of synthesis, it has very good dielectric properties and a good clarity.
- Emulsion polymerization, it involves the use of an emulsifying agent that creates micelles in which the polymerization of the monomer takes place. It has a very fine particle size (d=0.1 µm) and is used for special processes such as coating to produce items such as wallpaper and vinyl flooring, among others.
- Suspension polymerization

Suspension polymerization consists of keeping the monomer dispersed in water through stirring in the presence of surfactants; with the addition of the initiator, each drop of monomer polymerizes separately and is transformed into a polymer bead, which is recovered by filtration and drying. Suspension PVC is used in most PVC articles (80% of the total consumed). Cables, window profiles, technical profiles, pipes, etc. are produced using suspension PVC.

1.3 PVC THERMAL DEGRADATION

Non-stabilized PVC undergoes nonoxidative thermal degradation when exposed to temperatures equal to or exceeding 100°C [36]. This mechanism is widely acknowledged as a cage reaction, involving distinct stages of initiation, propagation, and termination. The primary initiators of this degradation, and therefore the main contributors to its thermal instability, are believed to be structural defects within the PVC material. These defects may originate during the polymerization process or arise during subsequent heating of the polymer, the main ones being tertiary chlorides and allylic chlorides [10, 36]. In the initiation phase, typically through dehydrochlorination, the release of HCl leads to the formation of such structural defects within the polymer, which becomes inherently thermally unstable. Subsequently, in the propagation stage, these groups swiftly extend into polyenes as dehydrochlorination advances, in a cage reaction called zip elimination. This process is catalyzed by the presence of HCl, resulting in the sequential elimination of HCl. The polymer, initially colorless, transitions to yellow to black, depending on the amount of double bonds formed.

Termination occurs through the following competing secondary reactions from the polyene sequences:

- Crosslinking of the polymer matrix, by intermolecular Dies-Alder cyclization and Friedel-Craft alkylation. These reactions not only affect the compound's discoloration but also elevate the viscosity of the polymer melt, resulting in a significant temperature increase.
- Emission of benzene through intramolecular reactions between cis-trans sequences, leading to the release of approximately 1 mole of benzene per 100 moles of HCl.

Three mechanisms have been proposed so far to describe the PVC thermal degradation:

- Radical, proposed in the 1950s, it does not account for the selectivity of the zip elimination and for the catalytic activity of HCl on the PVC thermal degradation.
- six-center concerted, proposed in 1980 and subsequently modified by Bacaloglu and Fisher [15], it provides an explanation for the catalytic activity of HCl and for

the selectivity of the zip elimination. The mechanism was dismantled by Starnes through a series of demonstrations in the 1990s and early 2000s.

- ionic/quasi-ionic, as of now, it stands as the most widely accepted explanation within the scientific community [16,17,36].

Nowadays, most researchers investigating the thermal dehydrochlorination of PVC accept a mechanism for polyene propagation that involves ion pairs or a highly polarized (quasi-ionic) four-center transition state.

The ionic mechanism, shown in Figure 1.3, involves the random formation of ion pairs throughout the polymer chain, particularly involving allylic chlorides due to their weaker bonds. An elimination reaction follows, where the chloride ion attacks methylene hydrogens, resulting in the creation of a double bond and the release of HCl. This process can produce between 14 and 20 polyene sequences before stopping [16].

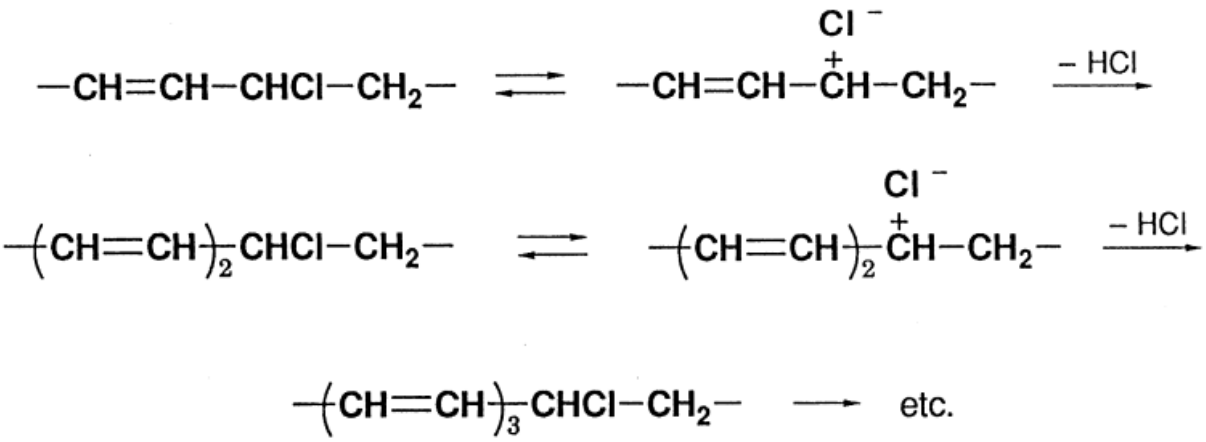

***Figure 1.3**: ionic mechanism for polyene sequences growth.*

The quasi-ionic mechanism is shown in Figure 1.4 [17].

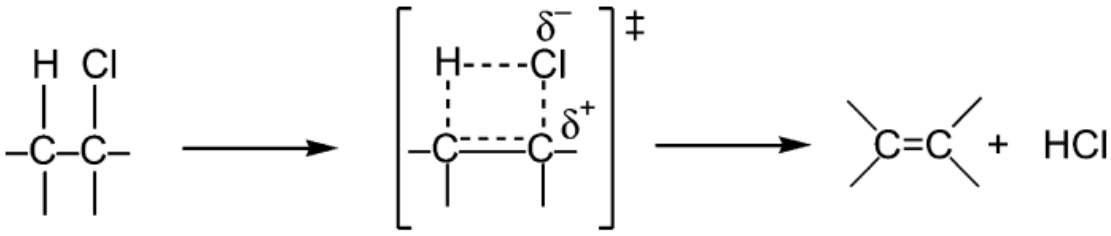

***Figure 1.4**: quasi-ionic mechanism*

It involves the concerted loss of HCl in a single step via a four-center transition state, which features a significant amount of charge separation in the breaking C–Cl bond.

The catalysis of dehydrochlorination by HCl, a well-established phenomenon, can be effectively explained by both the ion-pair mechanism and the concerted process. HCl reacts with already formed polyene sequences (PES), generating cationic polyene radicals, which then remove a methylene hydrogen from another section of the chain or from a neighboring chain in the polymer matrix. Consequently, through a β-elimination, new allylic chlorides are formed, resulting in new structural defects from which the ionic degradation can extend catastrophically throughout the polymer matrix. [18]

A scheme of the thermal degradation process of PVC compounds is depicted in Figure 1.5.

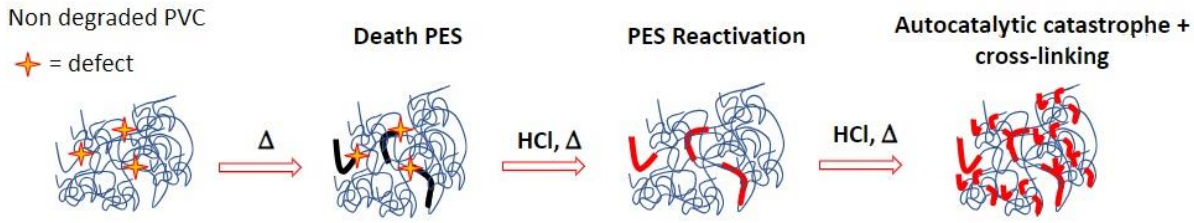

***Figure 1.5**: Thermal Degradation of PVC compounds.*

Similar to HCl, Lewis acids also catalyze the degradation of PVC. Consequently, a category of additives known as thermal stabilizers is critically important in PVC formulations.

1.4 PVC THERMAL STABILIZERS

To undergo processing at the required temperatures and be molded into articles, PVC needs the incorporation of diverse additives. These additives include thermal stabilizers, lubricants, plasticizers, fillers, process aids, and more.

The definition of plasticizers established by IUPAC back in 1951 remains widely acknowledged: it refers to a substance or material incorporated into another material, typically a plastic or elastomer, to enhance its flexibility, workability, or distensibility. Plasticizers can reduce melt viscosity, lower the temperature of a second-order transition, or decrease the elastic modulus of a product. For PVC, practical requirements for an effective plasticizer include cost-effectiveness, stability, minimal coloration, compatibility with PVC, easy dispersibility, low volatility, faint odor, low toxicity, good permanence, and the absence of adverse interactions with other formulation ingredients or the end-use properties of the product. The most important are phthalates, trimellitates, citrates, adipates, terephthalates, benzoates, and epoxy esters.

Lubricants are incorporated into PVC compounds to lower the degradation due to mechanical shear forces applied during processing, and the increase of the temperature. Among the most frequently used, there are polyethylene waxes, Fischer-Tropsch waxes, certain carboxylic acids like stearic and oleic acids, as well as specific carboxylic acid esters, and others.

The most widely used fillers in flexible and semi-rigid PVC are various grades of calcium carbonate, which can be derived from limestone or marble and processed through dry-ground, wet-ground, or precipitation methods. But also, functional fillers with flame retardant properties such as $Al(OH)_3$ (ATH) and $Mg(OH)_2$ (MDH) can be employed. Flame retardants such as Sb_2O_3 (ATO), medium-chain chlorinated paraffins (MCCP), brominated compounds, zinc borate, etc. can also be added.

Thermal stabilizers serve the crucial function of retarding the thermal degradation of PVC, ensuring the integrity of flexible PVC compositions during processing and shaping into final products, and can be divided into primary and secondary stabilizers. In a broad sense, the mechanism of a primary thermal stabilizer addresses the labile

allylic chlorine, displacing it through an entering group which forms a stronger bond, as depicted in Figure 1.6.

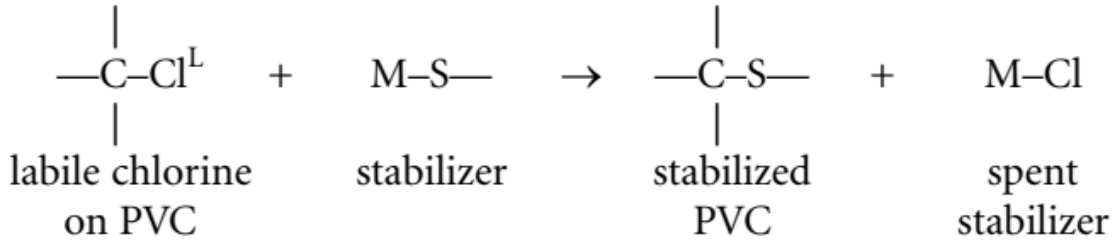

***Figure 1.6**: mechanism of primary thermal stabilizers. [13]*

Secondary stabilizers are a group of substances that help the allylic chlorine displacement, deactivate HCl and Lewis acids, repair polyene sequences and trap the radicals responsible for creating new defects. In some cases, a single molecule can fulfill the roles typically attributed to both "primary" and "secondary" stabilizers.
As for the desired attributes of stabilizers for flexible PVC, they ideally should have qualities such as being colorless, odorless, non-toxic, non-hygroscopic, non-volatile, non-conductive, resistant to oxidation and hydrolysis. Additionally, they should be cost-effective, shelf-stable, readily available, easily dispersible in PVC, compatible with PVC and other additives, stable to heat and light, easily processable, and efficient in their stabilizing function.
Based on the chemistry of the primary stabilizer, stabilizers can be divided into:

- Tin stabilizers
- Lead stabilizers
- Cadmium stabilizers
- Barium-zinc stabilizers
- Calcium-zinc stabilizers
- Organic stabilizers

Initially, lead-based stabilizer systems emerged as the pioneering solution for PVC, demonstrating commercial viability. In 2003, Directive 2002/95/EC (RoHS I) [19] banned cadmium and lead stabilizers in Electrical and Electronic Equipment (EEE), leading to their removal from all PVC cables. By December 2015, ESPA had completed the substitution of lead-based stabilizers in Europe, concluding the "VINYL 2010" initiative [20]. The EU began gradually eliminating cadmium-based liquid and

solid stabilizers in the mid-'90s after the Council Directive 91/338/EEC was enacted on June 18, 1991. This directive, which amended Directive 76/769/EEC, sought to limit the use of cadmium stabilizers and pigments in a wide range of products, such as packaging, containers, office supplies, clothing, textiles, flooring materials, pipes, vehicle interiors, and electrical wire insulation. As part of the Vinyl 2010 initiative, cadmium stabilizers were completely phased out in the EU-15 by 2001 and in the EU-27 by the end of 2007. [20]

Some tin stabilizers, made of organotin compounds, are under scrutiny by ECHA for, among others, reproductive toxicity, with potential removal from the EU market. [40]

Currently, Calcium Zinc, Barium Zinc, and Organic Stabilizers are the only types with a future perspective in the EU. Among these, solid Calcium Zinc and Organic stabilizers (COS) stand out as the most innovative solutions for the thermal stabilization of PVC.

To illustrate, let's examine the stabilization mechanism in PVC utilizing the calcium stearate - zinc stearate pair. Initially, zinc stearate functions as the primary stabilizer, displacing labile chloride groups (see Figure 1.7, reaction a). This displacement process replaces two allylic chlorides, yielding two molecules of $ZnCl_2$. Additionally, zinc stearate serves as an acid scavenger, generating $ZnCl_2$ (refer to Figure 1.7, reaction d). The $ZnCl_2$ formed in reactions a and d catalyzes PVC degradation as outlined in reaction b. Conversely, calcium stearate (reaction e) deactivates both $ZnCl_2$ and HCl, neutralizing their catalytic effects on PVC degradation and yielding $CaCl_2$, which is not a Lewis acid. Through reaction e, zinc stearate is effectively "regenerated" by calcium stearate, enabling its continued role as the primary stabilizer.

a

b

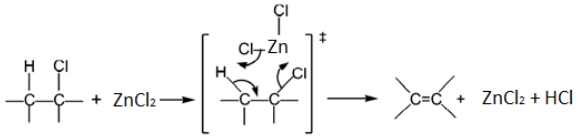

c

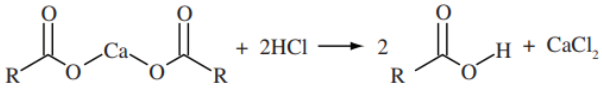

d

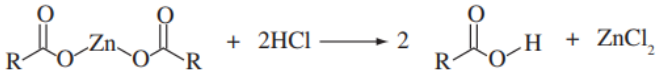

e

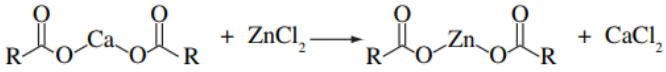

***Figure 1.7**: stabilization mechanism of PVC of the calcium stearate-zinc stearate pair.*

2 POLYMERS IN A FIRE

2.1 FIRE BEHAVIOR OF POLYMERS

Polymers, upon exposure to sufficient heat, undergo degradation and decomposition, liberating volatile substances into the surrounding environment. These volatile compounds, if reaching a critical concentration at sufficiently elevated temperatures, can ignite, initiating a flame. The ignition process is fueled by highly reactive radicals such as H• and OH• [41], which play a fundamental role in the exothermic chain reactions, including the oxidation of CO to CO_2. This phenomenon involves numerous species and reactions even for methane, the smallest among hydrocarbons, which combustion mechanism is depicted in Figure 2.1 [41], illustrating the radical reactions occurring within a hydrocarbon flame, which serves as a representative model for the combustion behavior of polymers.

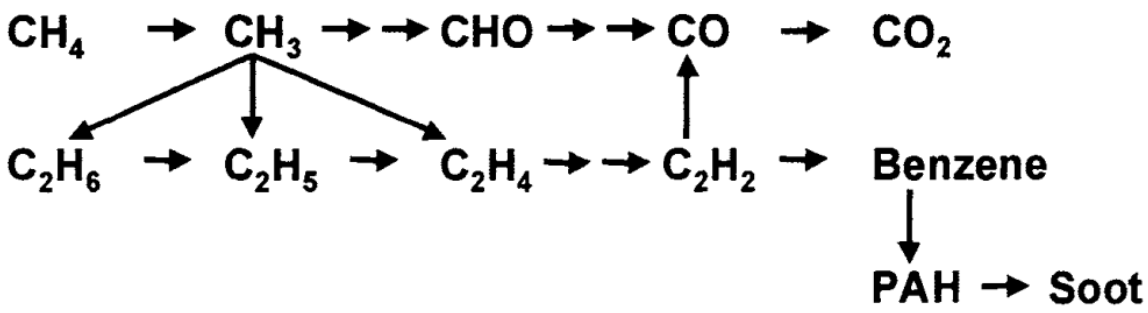

***Figure 2.1**: radical reactions in a combustion process of methane at high temperatures.*

Ignition can arise through spontaneous means (auto-ignition) or via an external ignition source such as a spark or flame (flash-ignition). Self-propagating occurs when the temperature, reached during combustion, is high enough to generate the

decomposition of the matrix which releases fuels burning in the air. That generates thermal feedback which sustains the combustion. [10]

Specifically in PVC compounds for cables, at temperature more than 220° C fuels can be yielded by the decomposition of PVC and some of its additives or additives' evaporation (e.g. plasticizers). [39]

Fires can be instigated by various sources, including plastics and other combustible materials like wood and paper found within a given environment. Plastics are ubiquitous in both fixed and non-fixed articles, permeating numerous aspects of modern living. However, if these plastic-containing articles are not adequately flame retarded, they pose significant risks in the event of a fire. The development of a fire within a compartment typically unfolds through four distinct stages [38], each characterized by specific phenomena and conditions:

- Incipient Stage: In this initial stage, combustion is not yet fully established, and the fire remains unstable. While ignition may have occurred, the fire has not yet gained significant momentum.
- Growth Stage: Following ignition, the fire gradually propagates within the compartment, accompanied by a progressive increase in temperature. During this stage, the fire remains manageable and extinguishable. Individuals in the vicinity can safely evacuate from the fire scenario.
- Fully Developed Stage: At the critical juncture of "flashover," typically occurring when temperatures soar to 600°C – 650°C, the entire contents of the compartment become engulfed in flames. This phenomenon results from the sudden ignition of gases released by the pyrolysis of materials. Rapid temperature escalation ensues, and the fire rapidly spreads to the entire compartment, marking the transition to the fully developed stage. At this point, the fire becomes uncontrollable and impossible to be extinguished using conventional methods.
- Decay Stage: The final phase of a fire, characterized by the diminishing thermal output as the fuel source is depleted. As the fire subsides, temperatures gradually decline. Once the temperature within the compartment

falls below 300°C, the fire is considered extinguished, marking the conclusion of the decay stage.

Understanding these sequential stages of fire development, depicted in Figure 2.2, is crucial for implementing effective fire safety measures, facilitating escape, and minimizing the risk of casualties and property damage.

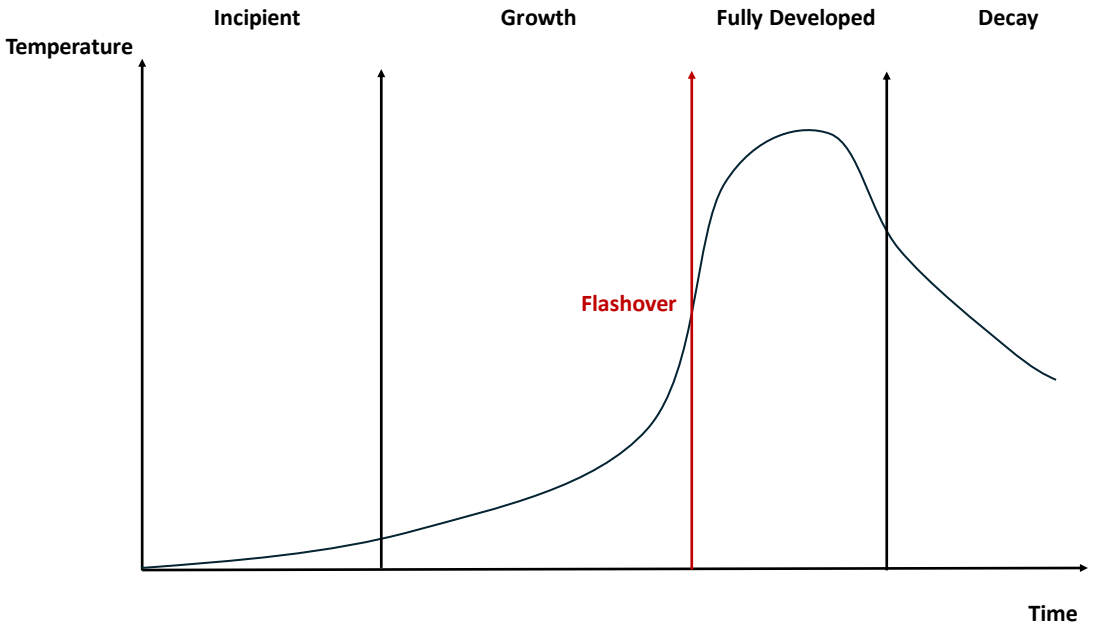

***Figure 2.2**: four stages of the fire development in a compartment.*

As noted, once "flashover" occurs, the opportunity to extinguish the fire is lost, leaving only the option to prevent its spread to adjacent areas. Most fatalities happen when fires grow uncontrollably and reach this critical point. Numerous studies have demonstrated that the most significant predictor of fire hazard is the heat release rate [7,9,11]. Therefore, it is crucial to use flame-retardant materials that can delay "flashover," thereby providing individuals with a greater chance to evacuate safely.

2.2 TEST AND REQUIREMENTS

In the evaluation of fire risks, the meticulous selection of materials with optimal fire performance stands as a critical determinant. The behavior of materials in fire scenarios is delineated by a spectrum of essential parameters, which include:

- Ease of extinction
- Flammability
- Flame spread
- Heat release
- Tendency to produce smoke and give obscuration
- Smoke Toxicity and acidity.

Ignitability, ease of ignition

The propensity of a material to ignite, characterized by its ease of ignition, plays a pivotal role in its contribution to fire propagation. Materials requiring substantial energy, and consequently, elevated temperatures to initiate flame ignition, tend to exhibit diminished involvement in fire incidents. To assess ease of ignition, many small-scale tests are available, among which cone calorimetry stands as a prominent method. Standardized tests such as ASTM E 1354 and ISO 5660 facilitate the evaluation of Time To Ignition (TTI), representing the duration for a material exposed to an energy source to sustain combustion. Within plastics, PVC and several PVC compounds notably demonstrate the highest TTI values, indicating their inherently reduced susceptibility to rapid flame initiation [13].

Ease of extinction

The ability of a material to ignite but subsequently extinguish the flame plays a crucial role in determining its contribution to fire spread. Materials that exhibit a high tendency to self-extinguish after ignition are crucial in limiting the escalation of fires. Evaluating the ease of flame extinction can be achieved through various small-scale tests, with the oxygen index test standing out as a prominent method. Standardized procedures such as ASTM D 2863 enable the determination of the Limiting Oxygen Index (LOI),

representing the minimum concentration of oxygen in a nitrogen-oxygen mixture required to sustain flaming combustion of a material.

Table 2.1 provides a comparative overview of LOI values for common plastics, highlighting PVC's position as one of the highest Oxygen Index values among polymers.

POLYMERS	LOI [%O_2]
FEP	96
PTFE	95
C-PVC	70
PVC	45
PC	26
NYLON 6.6	25
WOOL	25
EVA	19
PP	18
PE	17

Table 2.1: LOI value for the most common plastics.

Air composition can be simplified to a 79/21 nitrogen-oxygen mixture and plastics with a LOI below 21% are susceptible to combustion, propagating flames into the surrounding atmosphere. However, PVC exhibits inherent flame retardancy attributed to its chlorine content, significantly delaying flame development. Consequently, PVC demonstrates a high LOI value of approximately 45%. Conversely, the incorporation of general-purpose plasticizers, such as phthalic esters, significantly diminishes LOI values, as shown by data reported in Table 2.2. Consequently, the inclusion of flame retardants and smoke suppressants becomes imperative in flexible PVC compounds.

PVC 100, STAB 3, DIDP X (phr)	LOI [%O_2]
0	45
30	28

50	24
100	20

***Table 2.2**: LOI value for PVC formulations*

Flammability

Flammability, defined as the propensity of a material to ignite and burn with a flame [21], significantly influences its contribution to fire propagation. On a small scale, the UL 94 series test is widely employed to assess flammability, UL 94 for plastics comprises both vertical and horizontal test methods, each differing in severity. This standardized test involves igniting a specimen of specified thickness using a Bunsen burner, in accordance with procedures outlined in literature [30]. PVC compounds demonstrate notable performance in achieving stringent UL 94 ratings, particularly on thinner thicknesses [13]. A common apparatus to evaluate the flammability of materials is the MCC and the ASTM D 7309 provides two procedures to determine the flammability characteristics of materials in laboratory settings using controlled temperature programming and oxygen consumption calorimetry. [22]

Flame Spread

The propensity of a material to propagate a flame away from the fire source is crucial in assessing fire hazard. If a material tends to extend the "flame front" beyond the initial source of ignition, it significantly contributes to the spread of the fire to adjacent areas. The mechanisms driving flame propagation can be both physical and chemical. Physically, factors such as the shape and geometry of the material play a role. Chemically, the material's inherent properties, such as its ability to extinguish flames or, conversely, to facilitate the formation of burning droplets, influence flame spread.

There are numerous tests designed to evaluate flame spread, tailored to the specific articles being assessed. For instance, EN 50399 [23] is used to test vertically mounted bunched cables to determine their propensity to propagate the "flame front." This test is particularly relevant due to the length of cables and their potential to spread fire across different locations, posing a significant risk of large-scale fire propagation. Key parameters obtained from this test include Smoke Growth Rate (SMOGRA), Fire Growth Rate (FIGRA), and burn length.

Heat Release

Heat release, defined as the thermal energy generated during combustion, is a crucial factor in fire dynamics [21]. When a substance undergoes combustion, the heat released and its rate, plays a significant role in elevating the temperature of the environment and potentially igniting adjacent materials, before heat can be dissipated by colder air. Consequently, the measurement of a material's heat release rate (HRR), its peak (pHRR), and time (TTP), and the total heat release (THR) are fundamental parameters for assessing the potential size and intensity of a fire [17].

ISO has adopted the Cone Calorimeter as its bench-scale method (ISO 5660) for measuring Heat Release Rate [25]. The ASTM sibling is ASTM E 1354. The Cone Calorimeter is designed to simultaneously measure not only the heat release rate but also ignitability, smoke production, and the emission of various gas species, among other, CO, CO_2 and HCl.

Tendency to produce smoke and give obscuration

Obscuration from smoke in fires is a significant risk, as it limits both escape from the fire and rescue operations by safety personnel. It is influenced by two main factors: the amount of material burned in the fire (fire load) and the quantity of smoke released per unit mass. There are many standards for measuring smoke density (ASTM D 2843, ASTM E 1354 etc.). The primary method for evaluating smoke generated by burning materials on a small scale is the traditional NBS smoke chamber, typically operated in vertical mode according to ASTM E662 standards [24]. This apparatus measures the specific optical density of smoke emitted from a flat plastic sample (up to 25 mm thick) exposed vertically to radiant heat within an enclosed chamber, with or without a pilot flame. A sensor is used to measure the density of smoke collected during the specimen's combustion. PVC compounds, without smoke suppressants, tend to produce dense, dark smoke, especially when antimony trioxide is used as a flame retardant.

Smoke toxicity and acidity

The importance of smoke toxicity in relation to fire hazard and the emission of acid gases is often misunderstood. While it is true that approximately two-thirds of fire

fatalities are directly attributable to smoke toxicity, these deaths are rarely caused by the inhalation of smoke from a particularly toxic material. In fact, it is estimated that well over 90% of fire-related deaths result from fires growing too large and producing excessive amounts of toxic smoke. There is a strong correlation between high blood CO concentrations in fire victims and fatalities, indicating that the toxic effects of other combustion products are negligible in comparison. Consequently, the primary driver of fire hazard is the fire's HRR, which determines the fire's intensity. Other factors, such as smoke toxicity, are of lesser importance [11].

The toxicity of smoke in a fire is determined by four key factors: the quantity of materials burned, the distribution of combustion products within the smoke, the individual toxic potencies of each combustion product found in the vapor phase, and the duration of exposure [9]. At flashover, virtually all polymers will emit approximately 20% of their weight as CO, which is toxic enough to be lethal. Consequently, the smoke from fires that have reached flashover inherently contains a baseline level of toxicity due to CO. In this context, the toxicity of smoke from other fire effluents becomes relatively insignificant, as the amount of CO alone is enough to cause fatalities. Therefore, the primary concern regarding smoke toxicity at flashover is the concentration of CO, which establishes a critical threshold for the lethality of the smoke.

Halogenated polymers, particularly PVC, are the primary contributors to smoke acidity. When PVC undergoes combustion, it releases hydrogen chloride through zip-elimination, resulting in acidic smoke. Some researchers suggest that the acidity of the fumes can induce panic and hinder the escape a fire scenario, in 1985 Kaplan et al. [37] reported that lethal doses of irritants did not alter the efficiency of escape of rats and baboons. Additionally, HCl from small fires has the potential to corrode nearby electronic devices, but among the effluents it is not the only substance capable of such phenomenon [9]. Beitel et al. demonstrated that despite the initial release of HCl during combustion, accounting for only the 35% of the total chlorine content in the original PVC, gaseous HCl rapidly decays in the surrounding environment. For instance, water vapor from ambient humidity, which is a major combustion product of nearly all fuels, combines with HCl, leading to a decrease in its concentration in the atmosphere. So, it was observed that HCl was produced, reached a peak concentration, and then decayed, while other gases like CO, CO_2,

and hydrocarbons continued to increase. Furthermore, HCl did not travel from the location of combustion unless mechanically transported by a simulated air conditioning system. Considering all of this, most of the fire scientists claim that smoke acidity is a secondary concern compared to heat release and smoke density and CO.

2.3 FIRE BEHAVIOUR OF PVC COMPOUND

The fire performance of building and construction products is a critical aspect in fire safety. Thanks to chlorine, PVC has an inherent flame retardancy, even in the absence of additional flame retardants. Even PVC-P, when with the use of specific additives, can enhance its fire performance, at levels comparable to PVC-U. The key to PVC's exceptional fire performance lies in its release of HCl during combustion, which plays a fundamental role in suppressing the flame by trapping H• and OH• radicals, the primary agents responsible for flame propagation [26]. The release of HCl is also effective in promoting char formation in fires. Char forms a protective outer layer, inhibiting the spread of flames, smoke, and burning droplets. Moreover, unlike certain odorless toxic gases like CO, which pose significant hazards in fires, the presence of hydrogen chloride resulting from PVC combustion emits a distinct odor. Even at trace levels, the detection of HCl gas serves as an early warning signal for evacuation, ensuring the safety of occupants by alerting them to the presence of fire [9].

The fire behavior of PVC compounds is significantly influenced by the presence of Lewis acids, which not only catalyze PVC degradation by promoting zip-elimination but also act as smoke suppressant by leading to the formation of trans-polyene sequences, facilitating cross-linking reactions (such as Diels-Alder and Friedel-Craft) of polyene sequences. Conversely, in the absence of Lewis acids, intramolecular reactions are favored, thus promoting benzene and smoke production. Figure 2.3 illustrates the degradation pattern of PVC in the presence or absence of Lewis acids

within the formulation. [34]

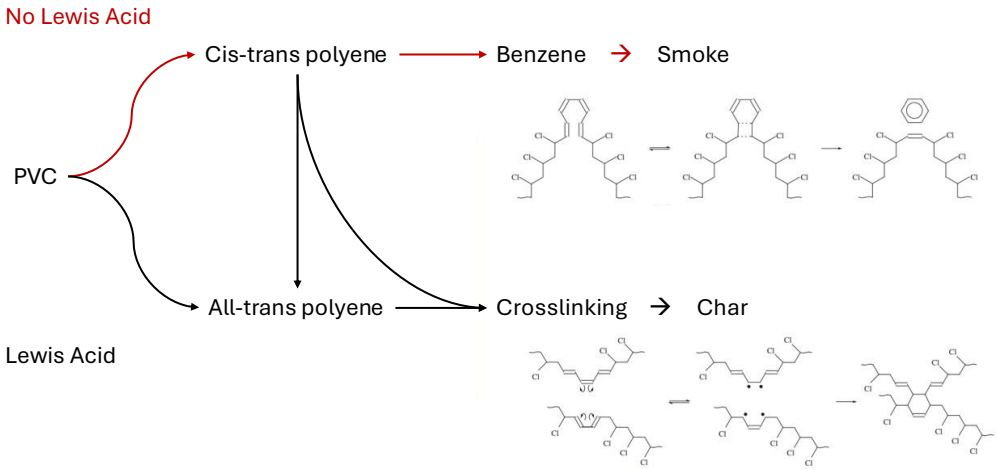

***Figure 2.3**: PVC degradation scheme.*

2.4 FLAME RETARDANTS AND SMOKE SUPPRESSANTS FOR PVC

As mentioned, PVC is inherently flame-retardant. However, the addition of certain additives, such as general-purpose plasticizers, can increase its tendency to burn and promote smoke production. The fire properties of plasticized PVC, which is commonly used in cable production, are largely determined by the type and amount of plasticizer added.

Flame retardants can work on a physical and a chemical approach, acting in the condensed or the gas phase. Some of them can be also remarkable smoke suppressants. Figure 2.4 illustrates the potential modes of action of flame retardants and smoke suppressants in both the gas and condensed phases.

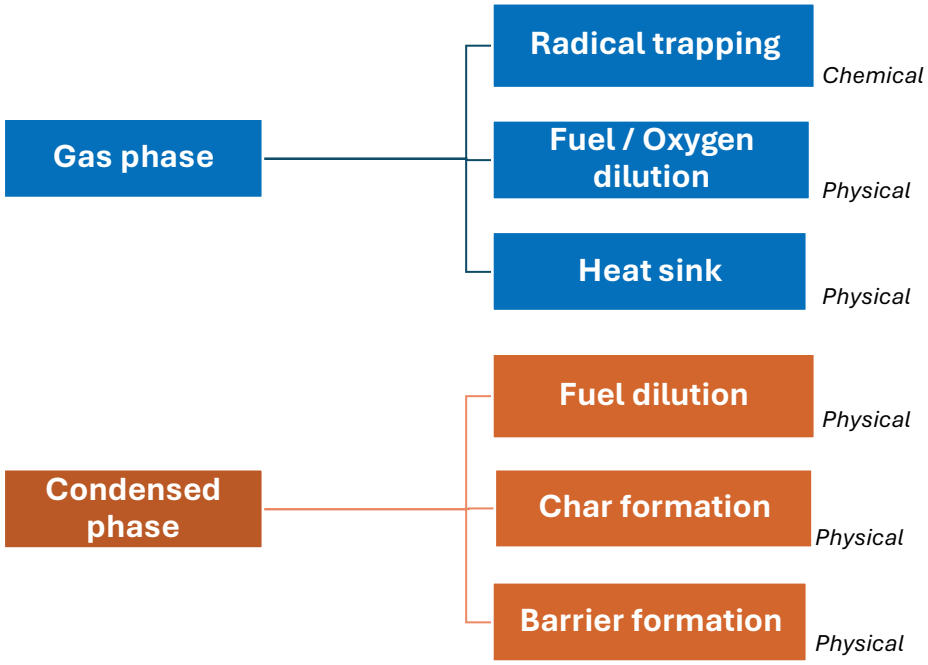

***Figure 2.4**: possibility of action of flame retardants and smoke suppressants.*

Additionally, Table 2.3 outlines the mechanisms of action of various flame retardants and smoke suppressants available in the market.

Additive	Mechanism of action	Explanation of mechanism	Drawbacks and Limitations
Chloroparaffins	*Radical Trapping*	The highly reactive radicals HO and H react in the gas phase with other radicals, such as halogenated ones from flame retardant degradation, slowing the combustion kinetics.	Lowers the thermal stability of the compound.

ATO	*Radical Trapping*	Synergistic effects between halogenated compounds and ATO, forming volatile antimony species that react with H• radicals, inhibiting combustion.	Leads to partial combustion, producing smoke and increasing [CO].
Lewis Acids [ex. ZnO, $ZnMoO_4$, Ammonium Octamolybdate)]	*Char Formation*	Formation of a carbonaceous layer by cross-linking of polyene sequences through Diels-Alder and Friedel-Crafts reactions catalyzed by Lewis Acids.	Lowers the thermal stability of the compound.
Organophosphates	*Radical Trapping* *Char Formation*	Act in the condensed phase by catalyzing char formation and diluting the fuel, and in the gas phase by using PO• and HPO• radicals as scavengers.	Some compounds produce smoke while burning
Metal Hydroxides	*Heat Removal* *Physical Barrier* *Fuel Dilution*	Their degradation is endothermic, leading to heat absorption. Produces water vapors that dilute combustible gases and forms an oxide layer protecting the material.	Basic compounds may cause discoloration of the compound

***Table 2.3**: mechanism of actions of the main smoke suppressants and flame retardants.*

2.5 ACID SCAVENGERS

To comprehend how HCl scavenging occurs in the condensed phase, it is crucial to examine the degradation mechanisms of PVC and PVC compounds during combustion. Among the various models proposed, the two-stage model for PVC resin puts forth by Wu is the most widely accepted within the scientific community [27, 39]. According to this model, the decomposition process of PVC under the experimental conditions consists of two distinct stages:

- Stage 1: it is characterized by the thermal dehydrochlorination of PVC resin which occurs between 220 °C and 350°C, releasing HCl (major product) and benzene in the gas phase and polyene sequences and their condensation products in the condensed phase.
- Stage 2. it is characterized by breakdown of the condensation products, releasing mainly aliphatic hydrocarbons and hydrogen and yielding a black mass called char.

The decomposition of a PVC compound is considerably more complex due to the presence of various additives that can interact with the released HCl, evaporate, or decompose.

- During the first decomposition step, PVC along with its organic and inorganic additives break down through a pyrolysis process in low-oxygen conditions. The predominant gas released at this stage is HCl, which results from the thermal decomposition of PVC itself, nonetheless the specific components of the PVC mixture determine the types and amounts of gases emitted during this breakdown. Various organic substances, including plasticizers, stabilizers, co-stabilizers, lubricants, and processing aids, can volatilize and combust, increasing both the heat output and smoke production. On the contrary, certain additives like flame retardant fillers release water vapor as they decompose, which absorbs heat and reduces fuel concentration, thereby lowering the flame's intensity. Additionally, side reactions between HCl and additives like calcium or magnesium carbonate can produce gases like CO_2, further weakening the flame. In the condensed phase, polyene sequences formed

during zip elimination can react intramolecularly (cis-olefinic), producing benzene or intermolecularly (trans-olefinic), forming cross-linked structures. HCl reacts with incipient Lewis acids in PVC smoke suppressants to form active Lewis acids. These acids catalyze the formation of trans-olefinic structures, promoting cross-linking. [39]

- The second step in the decomposition process starts at temperatures above 450 °C, the breakdown products in PVC materials release volatile fuels, mainly aliphatic hydrocarbons, into the gas phase while a carbonaceous char forms in the condensed phase. The released fuels ignite, intensifying the flame's energy. However, the carbonaceous char acts as a barrier, limiting flame propagation by insulating and protecting the underlying material. The final step is characterized by a significant emission of CO_2, stemming from the decomposition of $CaCO_3$.

An effective acid scavenger, compliant with EN 60754-1 [28] and EN 60754-2 [29] standards, must efficiently absorb the maximum possible amount of HCl throughout the PVC combustion process. It needs to remain active through the Pyrolysis and Combustion Zones, forming stable reaction products from 360 °C up to the peak temperatures defined by the tests (e.g., 810 °C in EN 60754-1 and 965 °C in EN 60754-2).

The HCl scavenging process involves complex reactions characterized by a series of HCl "transfers" between the different components involved. A thorough understanding of the interactions between acid scavengers and the polymer matrix is essential for improving efficiency. Acid scavengers function primarily in two ways: either as thermal stabilizers, which include metal soaps, alkali and alkaline earth metal hydroxides, hydrotalcites, zeolites, and hydrocalumites, or as HCl absorbers designed for high-temperature applications. Most acid scavengers consist of formulations containing two or more high-temperature acid scavengers that function synergistically with the polymer over a broad temperature range. For instance, the combination of $Mg(OH)_2$ and PCC, precipitated calcium carbonate, exemplifies this approach. $Mg(OH)_2$ captures HCl, forming $MgCl_2$, which is hydrolytically unstable at high temperatures and releases HCl slowly in a broad range of temperatures between 400 – 600 °C. HCl is then captured by PCC with a higher efficiency. Fine calcium carbonates are among

the simplest examples of high-temperature acid scavengers, traditionally used in PVC to produce compounds with low smoke acidity for specific applications.

3 CABLES

3.1 PVC IN CABLES

Cables serve as indispensable components of modern society, facilitating crucial functions in communication, power transmission, transportation, and various industrial sectors. The absence of cables would significantly impede the operation of numerous modern conveniences and systems. Essentially, an electrical cable consists of an electrical conductor, typically made up of one or more twisted wires, which is then covered by layers of insulating materials. Additionally, cables may also include beddings, armoring, shields, and an outer protective jacket.

Beddings provide extra protection between the conductor and the surrounding materials, while armoring and shields and screeners offer defense against mechanical stress and electromagnetic interference. Lastly, the outer jacket acts as a sturdy shield against physical damage, moisture, and other environmental factors. An example of an electrical cable currently available in the italian market is reported in Figure 3.1.

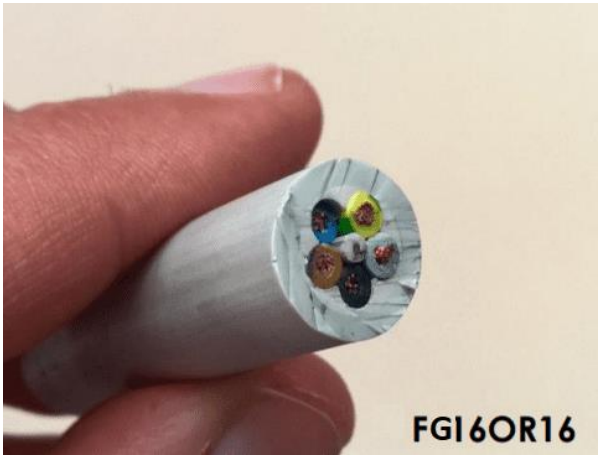

***Figure 3.1**: FG16OR16 G5X1.5 0.6/1.0 kV Italian electrical cable a.t. CEI UNEL 35016. [35]*

In most electrical cables, conductor wires employ metals known for their exceptionally low electrical resistivity, such as copper or aluminum. The thickness of the conductor is tailored to accommodate the current-carrying capacity and specific requirements,

whether for enhanced resistance to mechanical stress or increased flexibility. Insulation and sheathing materials are selected from a diverse array of thermoplastic and thermosetting polymeric options, including PVC, HEPR, NBR, XLPE, PE, CPE chloroprene, fluorinated polymers, silicones, nylon, and more.

In the EU, PVC compound for cables had a market share between 35 – 39 % in 2023 and therefore is yet the predominant plastic [31]. Renowned for its versatility, electrical insulation properties, inherent flame-retardancy, and cost-effectiveness, polyvinyl chloride is extensively employed in cable manufacturing. In terms of the sustainability of PVC material in cable formulations, it's crucial to emphasize the concerted efforts made by the entire PVC value chain over the past two decades. Their focus has been on enhancing sustainability not just in production processes, minimizing emissions and energy use, but also in the resulting products, investing more than €6 billion for the transition from SVHC low molecular weight phthalates to innovative non-SVHC phthalates and other plasticizers [33]. Furthermore, PVC cables exhibit ease of mechanical recycling, contributing to their high recycling rate across Europe. [14, 30]. Nonetheless, there has been a notable decrease in the use of PVC compounds for electrical and telecommunication cables in recent decades. This trend is largely driven by the adoption of halogen-free materials, which do not emit acidic smokes.[31] The graph in Figure 3.2 illustrates the decline in the consumption (in percentage) of PVC compound in the Global Cable Industry compared to other polymers [31].

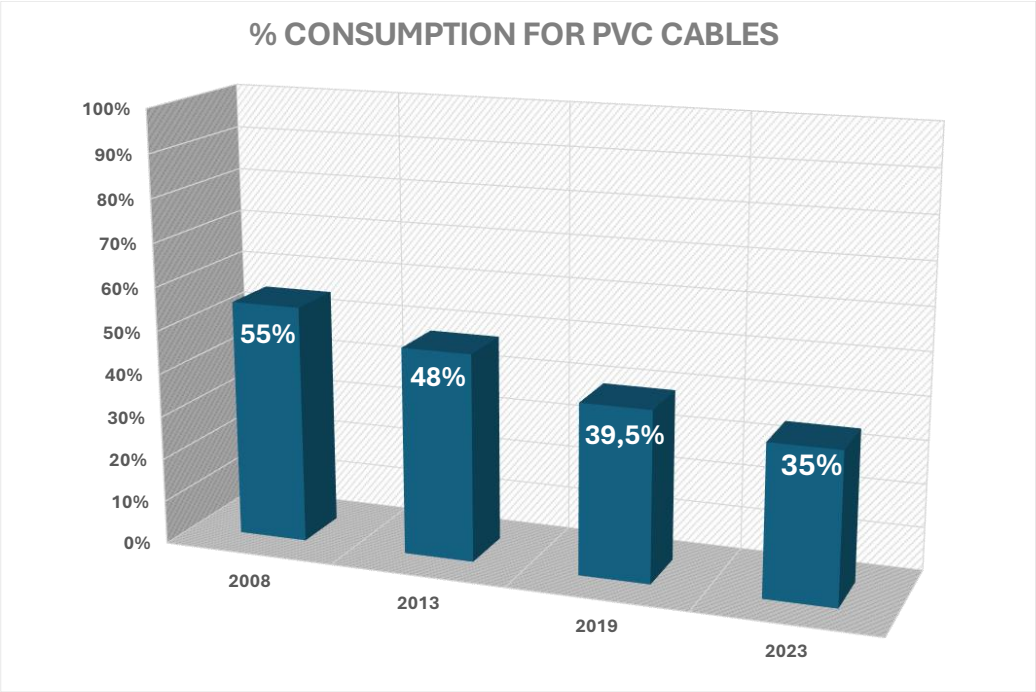

***Figure 3.2**: consumption (%) of PVC compounds for cables.*

3.2 REGULATIONS AND PVC CABLES

In the EU, the Construction Product Regulation (CPR), Regulation EU No. 305/2011, lays down harmonized conditions for the marketing of construction works. This regulation, which replaced Council Directive 89/106/EEC [32] (the Construction Product Directive, CPD) in 2017, aims to help the marketing of construction products within the EU. CPR achieves this by adopting standardized technical language that clearly defines the performance and essential characteristics of construction products, thereby minimizing risks to individuals and property.

Annex I of the CPR states the basic requirements for construction works, listing seven safety requirements. At the second point it is included safety in case of fire, in which it is reported as follows:

“The construction works must be designed and built in such a way that in the event of an outbreak of fire:

(a) the load-bearing capacity of the construction can be assumed for a specific period of time;

(b) the generation and spread of fire and smoke within the construction works are limited;

(c) the spread of fire to neighboring construction works is limited;

(d) occupants can leave the construction works or be rescued by other means;

(e) the safety of rescue teams is taken into consideration."

The CPR outlines several crucial elements to ensure safety in the event of fire. First, it establishes a harmonized classification system for construction products based on their fire performance. This system ensures consistency across different types of products and applications. Second, the CPR mandates common standards and requirements, promoting uniformity in safety measures across the EU. Third, it requires the use of standardized control procedures by competent authorities, ensuring that all products meet the necessary safety criteria.

A key aspect of CPR is the requirement for products to bear a CE marking. This marking signifies that the product has a Declaration of Performance (DoP), which certifies that the product meets all the specified performance standards. Without this declaration, the CE marking cannot be affixed. Electrical cables for fixed installations are categorized as building and construction products under the CPR. To ensure their compliance with fire safety standards, the CPR has enacted two specific technical standards that these cables must adhere to:

- EN 50575 [2]: This European Standard outlines the performance criteria, testing procedures, and evaluation methods for electric cables utilized in construction projects for electricity supply, control, and communication purposes. These cables are subject to stringent requirements regarding their reaction to fire. The cables addressed by this standard are specifically designed for electricity and communication applications within buildings and other civil engineering projects. The primary aim is to minimize the generation and dissemination of fire and smoke within these structures.

- EN 13501-6 [3]: The objective of this European Standard is to establish a standardized procedure for classifying the reaction to fire of electric cables and set standards and requirements to obtain such classes.

The European standard EN 13501-6 [3] categorizes electric cables into 7 reaction-to-fire classes from A to F, identified by the subscript 'ca' (cable), based on their performance in heat release and flame spread. These classes, along with their classification criteria and the corresponding standards used for assessment, are presented in Table 3.1.

Class	Test	Classification Criteria
Aca	EN ISO 1716	PCS ≤ 2,0 MJ/kg
B1ca	EN 50399	FS ≤ 1,75 m; THR 1200s ≤ 10 MJ; Peak HRR ≤ 20 kW; FIGRA ≤ 150 W/s
B2ca	EN 60332-1-2	H ≤ 425 mm
Cca	EN 50399	FS ≤ 2,0 m; THR 1200s ≤ 30 MJ; Peak HRR ≤ 60 kW; FIGRA ≤ 300 W/s
Dca	EN 50399	THR 1200s ≤ 70 MJ; Peak HRR ≤ 400 kW; FIGRA ≤ 1300 W/s
Dca	EN 60332-1-2	H ≤ 425 mm
Eca	EN 60332-1-2	H ≤ 425 mm
Fca	EN 60332-1-2	H > 425 mm

***Table 3.1**: classes for reaction- to-fire according to EN 13501-6.*

Each Member State incorporates this classification system into its own legislative framework addressing fire safety in buildings and constructions. It is important to acknowledge that the classification of a specific PVC cable may vary depending on its formulation and design, it is imperative to verify its classification to ensure compliance with the fire safety requirements of the intended use. Furthermore, in addition to the primary classes (A to F), the classification system also includes additional classifications that define performances such as smoke production (s), flaming droplets and/or particles (d), and acidity (a). Hence, the CPR establishes standardized classification criteria for cables across the EU. In Italy, as outlined by CEI UNEL 35016

[35], cables are categorized into four classifications based on their fire performance, outlined in Table 3.2.

CPR Class	Additional classes	Who?
B2ca	s1a d1 a1	LSZH
Cca	s1b d1 a1	LSZH
Cca	s3 d1 a3	PVC
Eca	none	PVC

***Table 3.2**: Italian classification for fire performance cables according to CEI UNEL 35016*

Depending on fire risk assessments conducted in compliance with the respective internal laws and codes of European countries, cables are selected following the principle of prioritizing "higher fire risk" and opting for "higher performance cables". Table 3.3 from [30] offers guidelines for cable selection based on their intended placement.

HIGHLY FREQUENTLY INTERCHANGE PLACES		**RAILWAYS**
▪ Railway and maritime stations ▪ Subways ▪ Terminals	HIGH RISK	
TRANSPORT AND COMMUNICATION		**GALLERIES AND PARKING LOTS**
▪ Railways ▪ Railway tunnels with a length of more than 1,000 m ▪ Road tunnels with a length exceeding 500 m ▪ Garages	HIGH RISK	
HEALTH FACILITIES		**HEALTH**
▪ Hospital and nursing homes with hospitalisation ▪ Assisted residences for the elderly and disabled ▪ Rehabilitation facilities	MEDIUM RISK	
ENTERTAINMENT, SHOW AND CULTURE		**ENTERTAINMENT**
▪ Cinemas, theatres, discos ▪ Sports centres and gyms ▪ Museums, galleries, exhibition spaces ▪ Exhibition areas ▪ Libraries ▪ Shopping centres	MEDIUM RISK	
SCHOOLS		**SCHOOLS**
▪ School buildings of every order and degree	MEDIUM RISK	
HIGH BUILDINGS		**HIGH BUILDINGS**
▪ Buildings for civil use with fire-fighting > 24 m to 28 m ▪ Companies and offices with over 300 people	MEDIUM RISK	
ACCOMMODATION FACILITIES		**HOTELS**
▪ Hotel, motel, guesthouses ▪ Tourist villages, holiday homes, campgrounds ▪ Student accommodation ▪ Holiday farms and bed & breakfast	MEDIUM RISK	
RESIDENTIAL BUILDINGS		**RESIDENCE**
▪ Houses and residential buildings < 24 m to 28 m ▪ Small companies, professional offices ▪ Shops, bars and restaurants	LOW RISK	

***Table 3.3**: cables classes according to the locations. [43]*

3.3 ADDITIONAL CLASSIFICATION FOR ACIDITY

As per the Construction Product Regulation, EN 60754-2 (Figure 3.3) is designated as the standard for assessing smoke acidity through tests conducted on gases emitted during the combustion of cable materials. Conversely, EN 60754-1 (Figure 3.4) serves as a standard specifically applied to PVC cables, operating outside the regulatory framework of the CPR. EN 60754-3 (Figure 3.5) utilizes the same test apparatus and procedures as EN 60754-2. However, Ion Chromatography is used to detect halogens.

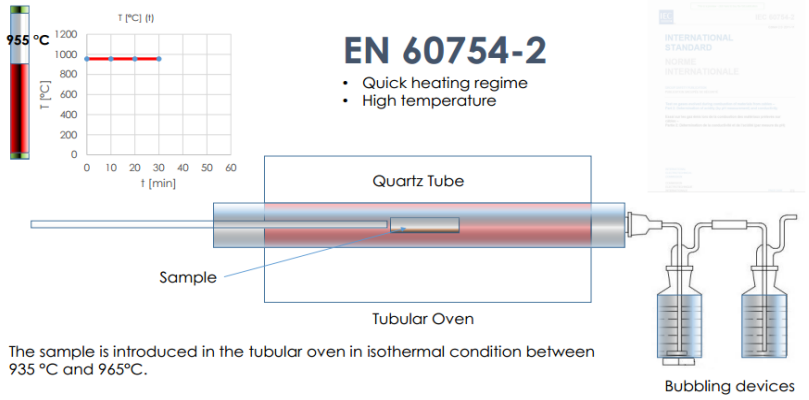

***Figure 3.3**: EN 60754-2.*

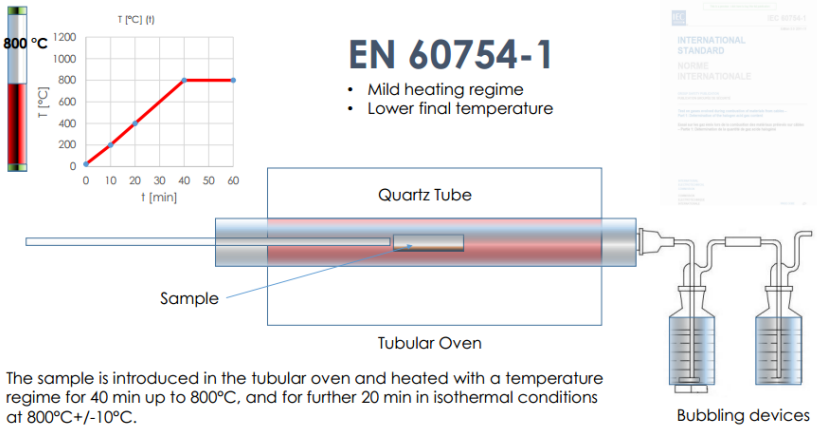

***Figure 3.4**: EN 60754-1.*

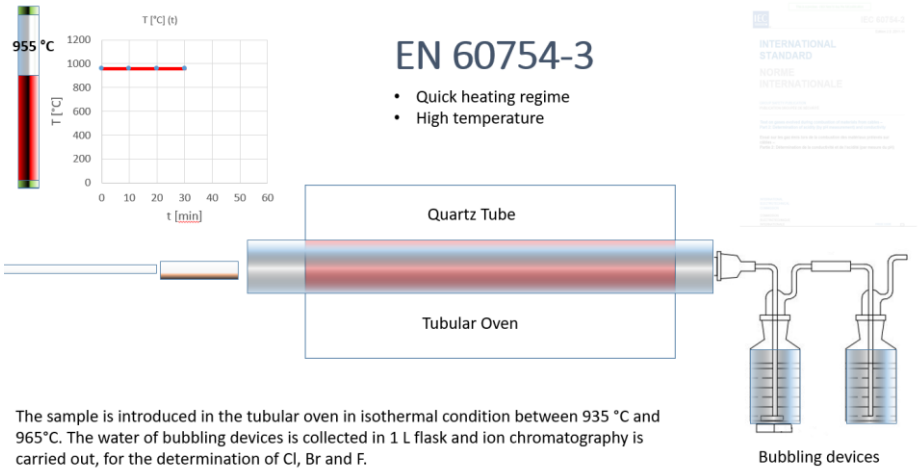

***Figure 3.5**: EN 60754-3.*

The Construction Products Regulation (CPR) defines the following classes of smoke acidity for cables:

- Class a1: pH > 4.3, Conductivity [mS/mm] < 2.5
- Class a2: pH > 4.3, Conductivity [mS/mm] < 10
- Class a3: pH ≤ 4.3, Conductivity [mS/mm] ≥ 10.

PURPOUSE OF THE THESIS

The objective of this thesis is to evaluate the fire performance of various compounds used in cable manufacturing, specifically for insulation, bedding, and jacket applications. The study focuses on PVC based compounds currently available on the market, including R16, S17, and PVC beddings, as well as low smoke acidity PVC counterparts developed by PVC4cables, and halogen-free alternatives. The primary aim is to assess the fire behavior of these materials using Cone Calorimetry at different incidental heat fluxes: 35 kW/m², representative of near-flashover conditions [8] (670 °C), and 62 kW/m², corresponding to a fully developed fire stage (825 °C). Additionally, Microscale Combustion Calorimetry was conducted to analyze the combustion and decomposition patterns of the different materials as a function of increasing temperature, described by specific heat release rate. LOI measurements were carried out to assess the materials' ease of extinction when exposed to fire, providing a quantitative value that allows for straightforward comparison between different formulations. The compounds under investigation are those employed in the production of CPR low voltage national Italian cables FG16OR16 and FS17 realized with PVC compounds, as well as their halogen-free counterparts, FG16OM16 and FG17.

4.RESULTS AND DISCUSSION

F50.8, R16, S17 and PVC BEDDING were prepared in the laboratories of Reagens Spa in San Giorgio di Piano (BO). General characterization was performed on these compounds to evaluate if they met the requirements for commercial applications. Formulations are presented in Table 4.1.

Raw Materials	**Trade Name**	**Company**	**PVC BEDDING (phr)**	**S17 (phr)**	**R16 (phr)**	**F50.8 (phr)**
PVC	Inovyn 271 PVC	Inovyn	100	100	100	100
DINP	Diplast N	Polynt	50		45	50
DIDP	Diplast RS	Polynt		46		
ESBO	Reaflex EP/6	Reagens	8			2
Antioxidant	Arenox A10	Reagens				0,1
Chloroparaffins	CERECLOR S52	Inovyn	20		15	
$CaCO_3$	Hydrocarb 95 T	Omya	150	60	30	
UUPCC	Winnofil S	Imerys				90
MDH	Ecopyren 3.5	Europiren	30		60	40
$MgCO_3$	MAGFY	Nuova Sima	150			
Caolino	SATINTONE SP 33	BASF		10		
ATO	RI004	Quimialmel	10	3	6	5
Zinc Borate	ZNB	Quimialmel	2			
COS	RPK B-CV/3038	Reagens	3,5	5	5	
COS	RPK B-CV/3037	Reagens				3

Lubricant	REALUBE PO	Reagens	0,5		0,5	
Lubricant	REALUBE RL 105	Reagens	0,4	0,1	0,4	
Lubricant	REALUBE PS	Reagens		0,3		

***Table 4.1**: Formulations PVC BEDDING, S17, R16 AND F50.8. Inovyn 271 PC is a suspension **PVC** with a K value of 71 from Inovyn. **DINP** means Di Iso Nonyl Phthalate; Diplast N is the trade name of Polynt S.p.A. **DIDP** means Di Iso Decyl Phthalate. **ESBO** stands for Epoxidized Soy Bean Oil. The used **antioxidant** is Arenox A10, a Reagens trade name, which is Pentaerythritol tetrakis(3-(3,5-di-tert-butyl-4-hydroxyphenyl)propionate), CAS number 6683-19-8. CERECLOR S52, medium chain chloroparaffin with a Cl percentage of 52%. **Zinc Borate** with different Zn/B/O/H ratios. REACH zinc borates are: ZnBHO3, CAS n 1332-07-6; Zn2B6O11, CAS n 12767-90-7. **COS** stands for calcium organic stabilizer. RPK B-CV/3037 and RPK B-CV/3038 are typical stabilizer for 70 °C cables produced by Reagens. Hydrocarb 95 T is groundmilled **calcium carbonates**, having a stearic acid coating and with a particle size distribution (D50) of 0.7 microns. Winnofil S is a **UUPCC** having nanoscale mean particle size. Ecopyren 3.5 is an uncoated ground-milled **MDH** produced by Europiren, with a D50 of 3.0 microns. MAGFY is **magnesium carbonate**, with a particle size distribution of 2.5 microns. SATINTONE SP 33, **Caolino** is a mineral, aluminum hydroxylicate. REALUBE PO, polyethylenic wax used as high temperature **lubricant.** REALUBE RL 105, Fischer-Tropsch wax used as high temperature **lubricant.** REALUBE PS, stearic acid used as low temperature **lubricant**. Formulations are expressed per hundred resin (phr).*

While M16, G16, G17, BEDDING_G, R16_LSA and PVC BEDDING_LSA were supplied by PVC4cables.

All compounds under analysis are reported in Table 4.2, which also depict a summary of the characterization carried out.

	F50.8	R16	R16_LSA	M16	G16	S17	G17	PVC BEDDING	PVC BEDDING_LSA	BEDDING_G
Hardness Test	×	×				×		×		
Tensile Test	×	×				×		×		
Plasticorder	×	×				×		×		
Colour Evaluation	×	×				×		×		
Relative Density	×	×				×		×		
Wener-Mathis Oven	×	×				×		×		
Thermal Stability	×	×	×			×		×		
MCC	×	×	×	×	×	×	×	×	×	×
LOI	×	×	×	×	×	×	×	×	×	×
Cone Calorimetry	×	×	×	×	×	×	×	×	×	×

***Table 4.2**: summary of the characterization.*

The compounds under investigation are those employed in the production of various cable geometries of national Italian cables, including FG16OR16 and FS17, as well as their halogen-free counterparts, FG16OM16 and FG17. FG16OR16 and FG16OM16 are multipolar power cables insulated with high-modulus ethylene propylene rubber, G16 quality. The first having PVC bedding and outer jacket of R16 quality, while the second one has HF counterparts as components of the cable. FS17 is a power cable insulated with PVC compound of S17 quality and FG17 has an HF insulation alternative. Graphical representations of such cable geometries are presented in Figure 4.1 and Figure 4.2.

***Figure 4.1**: FG16OM16 on the left, FG16OR16 on the right. [48]*

***Figure 4.2**: FG17 on the left, FS17 on the right. [48]*

These cables must meet the requirements to fit into the reaction fire class reported in Table 4.3 outlined by CEI UNEL 35016.

Cable geometry	Fire class	Smoke Class	Droplets class	Acidity Class
FG16OR16	C_{ca}	s_3	d_1	a_3
FG16OM16	C_{ca}	s_{1b}	d_1	a_1
FS17	C_{ca}	s_3	d_1	a_3
FG17	C_{ca}	s_{1b}	d_1	a_1

***Table 4.3**: reaction fire classes.*

PVC4cable obtained the reaction fire class $B_{2ca}\ s_1\ d_0\ a_3$ for FG16OR16 LSA, [46] manufactured using the R16_LSA and BEDDING_LSA under investigation in this thesis.

4.1. SAMPLES CHARACHTERIZATION

Table 4.3 shows a summary of the averages of the results obtained from general characterization.

Analysis	F50.8	R16	R16_LSA	S17	PVC_BEDDING
Hardness values	91.0	89.6		93.1	90.9
STRESS AT FAILURE, (MPa)	10,44 ± 0,45	15,05 ± 1,17	6,41 ± 0,70	16,08 ± 1,08	
STRESS AT FAILURE, (MPa) (AFTER AGING)	11,73 ± 0,38	15,98 ± 1,05	7,10 ± 0,44	16,92 ± 0,44	
Dryblend gelation time (s)	18	24		94	120
***L**	62.80	60.51		83.305	74.52
***a**	5.87	7.22		0.93	3.55
***b**	3.40	7.75		9.86	10.04
Density	1,579	1,529		1,460	1,860
Congo Red before aging (s)	75	65	206	142	78
Congo Red after aging (s)	72	63	176	112	72

***Table 4.3**: summary of the averages obtained from general characterization.*

4.1.1 Hardness Tests

All results from hardness measurements are reported in Table 4.4.

	AVERAGE	dev std.
R16	**89.6**	**0.8**
S17	**93.1**	**0.6**
PVC BEDDING	**90.9**	**0.6**
F50.8	**91.0**	**0.5**

***Table 4.4**: Average hardness values*

All compounds displayed similar hardness characteristics, the insulation of S17 quality presented the highest value among all compounds.

4.1.2 Tensile Test

Tensile tests were performed, before and after a period of aging at 100°C for 10 days, to assess if the prepared compounds met the requirements provided by CEI EN 50363-0 national annex [45], as outlined in Table 4.5. Results of tensile tests after aging must be in an interval of ± 25% regarding the ones obtained before aging.

The results obtained by the tensile analysis, before and after the aging process, are reported in Table 4.5 and Table 4.6.

	R16 LSA	R16	S17	F50.8
STRESS AT FAILURE, (MPa)	6,41 ± 0,70	15,05 ± 1,17	16,08 ± 1,08	10,44 ± 0,45
STRESS AT FAILURE, (MPa) (AFTER AGING)	7,10 ± 0,44	15,98 ± 1,05	16,92 ± 0,44	11,73 ± 0,38
Variation after aging (%)	+10	+6	+5	+11

Requirements CEI EN 50363-0 national annex (MPa) [before aging]	>12,5	>12,5	>15	>12,5

***Table 4.5**: Average of tensile test results ± st. dev.*

	R16 LSA	**R16**	**S17**	**F50.8**
ELONGATION AT FAILURE, (%)	130,00 ± 15,8	167,50 ± 18,9	180,00 ± 22,4	111,00 ± 16,9
ELONGATION AT FAILURE, (%) (AFTER AGING)	94,60 ± 1,9	132,00 ± 16,4	150,00 ± 10,0	68,50 ± 9,5
Variation after aging (%)	-37	-27	-20	-62
Requirements CEI EN 50363-0 national annex [before aging]	>150	>150	>150	>150

***Table 4.6**: Average of tensile test results ± st. dev.*

As anticipated, the inclusion of fillers reduces the material's elasticity, resulting in a product that is "harder" and more brittle. This leads to lower tensile strength and reduced elongation at break. The compounds subjected to the standard are those used for the jacket and insulation. As a result, only the samples R16, F50.8, and S17 were subjected to aging at 100°C, with R16 LSA also included for comparison with R16. The mechanical requirements necessary for certifying an electrical cable are

outlined in the CEI EN 50363-0 national annex [45]. R16 LSA and FR50.8 did not meet the specifications due to suboptimal gelation during lab preparation. However, R16 LSA has been certified under the CEI EN 50363-0 national annex [45]. Of the two jacket compounds prepared at Reagens, only R16 met the requirements for both tensile strength and elongation at break. The S17 compound also fulfilled the requirements set by the standard.

4.1.3 Rheology

The plastogram is a graph that depicts torque [Nm] over elapsed time. Figure 4.3 presents plastograms obtained from tests on F50.8, R16, PVC BEDDING and S17.

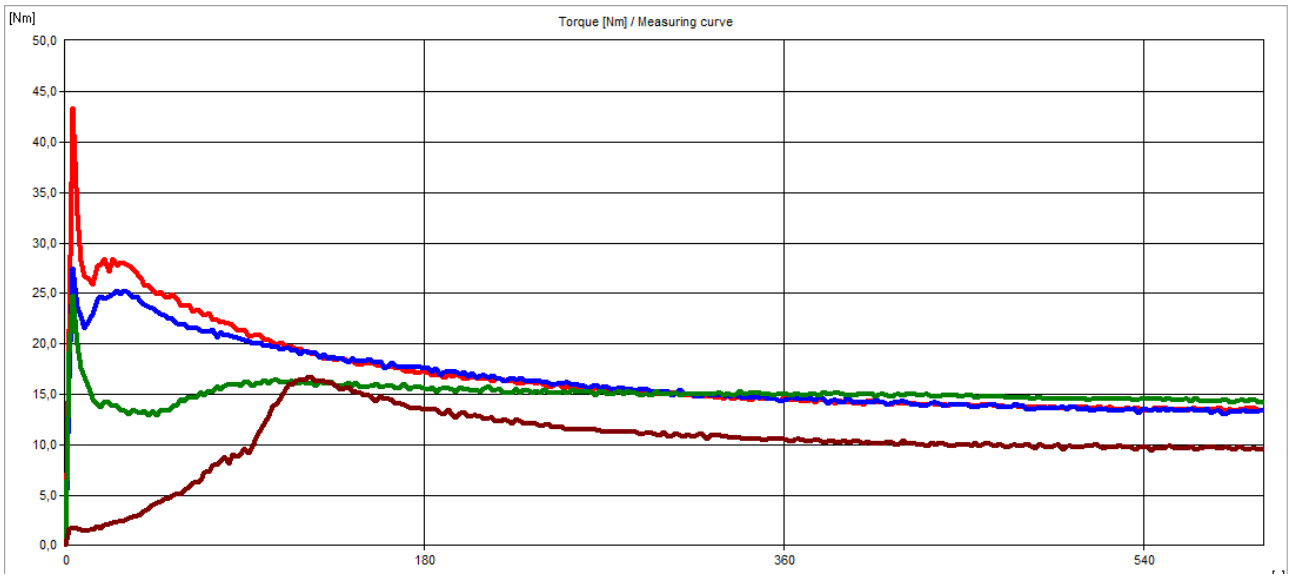

***Figure 4.3**: plastograms of R16 (blue), F50.8 (red), S17 (green) and PVC BEDDING (wine).*

Each curve has a distinct peak (point A), where the torque reaches its highest value when the dryblend is loaded and the ram and weight are applied. This is followed by a point of minimum torque (B), indicating the early stages of gelation. Subsequently, there is a relative maximum (point X), representing the completion of dryblend gelation. The fusion time is determined by the interval between point A and point X.

All results obtained are reported in Table 4.7.

	F50.8		S17		R16		BEDDING	
	Time (s)	Torque (Nm)	Time (s)	Torque (Nm)	Time (s)	Torque (Nm)	Time (s)	Torque (Nm)
A	4	43.4	4	24.9	4	27.5	2	1.7
B	12	26.5	42	12.9	12	22.4	62	5.8
X	22	28.5	98	16.1	28	25	122	16.8
A-X	**18**	-	**94**	-	**24**	-	**120**	-

***Table 4.7**: Plasticorder measurements results.*

We can observe as expected that the PVC BEDDING, owing to its high content of filler in respect to the amount of plasticizer, exhibits a higher time of gelation and a lower viscosity than all other compounds. While the jackets demonstrated the highest values of viscosity, confirming the trend of highest viscosity for greater volumes of plasticizer.

The plasticorder is useful to assure a homogeneous processing of the dryblend, so to obtain kneaders, suitable samples for other measurements like Congo Red and MCC.

4.1.4 Colour Evaluation

The results of the colorimetric analysis are reported in Table 4.8.

Colour	R16	F50.8	PVC BEDDING	S17
***L**	60.51	62.80	74.52	83.305
***a**	7.22	5.87	3.55	0.93
***b**	7.75	3.40	10.04	9.86

***Table 4.8**: Results of colorimetric analysis.*

The R16 and the F50.8 compounds exhibited a visual defect named "pinking," a known issue in PVC products when great amounts of basic components like $Mg(OH)_2$ and $Ca(OH)_2$ are included in the formulations. At typical processing

temperatures, these additives promote the formation of conjugated polyene sequences (PES) with 14-20 double bonds, which absorb light in the green region of the spectrum, giving the material a pink or reddish tone. Normally, the presence of these species has an impact on the aspect of the article but does not affect the mechanical and fire resistance properties of the item since their concentration is very low. [47]

4.1.5 Relative Density

The results are presented in Table 4.9.

	R16	PVC BEDDING	S17	F50.8
Density [g/mL]	1,529 ± 0,004	1,860 ± 0,003	1,460 ± 0,006	1,579 ± 0,004

***Table 4.9**: Average of the relative density values ± st. dev.*

The presence of fillers is directly correlated with an increase in the compound's density. As expected, the PVC BEDDING formulation exhibited the highest density value due to its higher filler content, while the S17 compound showed the lowest density among the tested samples.

4.1.6 Thermal stability

Specimens were evaluated both before and after aging, with the results presented in Table 4.10 and Table 4.11.

Congo Red	R16	F50.8	PVC BEDDING	S17	R16 LSA Inverplast
Average(s)	65	75	78	142	206
10%	58	67	70	128	185
-10%	71	82	86	156	227

***Table 4.10**: Average of Congo Red values before aging.*

Congo Red	R16	F50.8	PVC BEDDING	S17	R16 LSA Inverplast
Average(s)	63	72	72	112	176
10%	57	65	65	101	158
-10%	70	80	80	124	193

***Table 4.11**: Average of Congo Red values after aging.*

The slight reduction in the time required for the various compounds to release HCl after aging is due to the fact that a portion of the thermal stabilizer has already reacted with the HCl released during oven exposure. A significant difference can be observed between R16 and R16 LSA; the presence of acid scavengers in R16 LSA greatly limits the release of HCl. The F50.8 compound shows a similar average HCl release time to R16, this outcome can be explained by the fact that the acid scavenger in F50.8, WINNOFIL S, is only effective at high temperatures above 200°C, whereas the CR test is performed at exactly that temperature, limiting its effectiveness during the test.

Comparing the R16 compound with S17, both PVC-based, reveals a notable difference in thermal stability, which can be attributed to their differing formulations. R16 contains chloroparaffin, which is absent in S17.

4.1.7 Werner-Mathis Oven

The specimens after the process are presented in Figure 4.4.

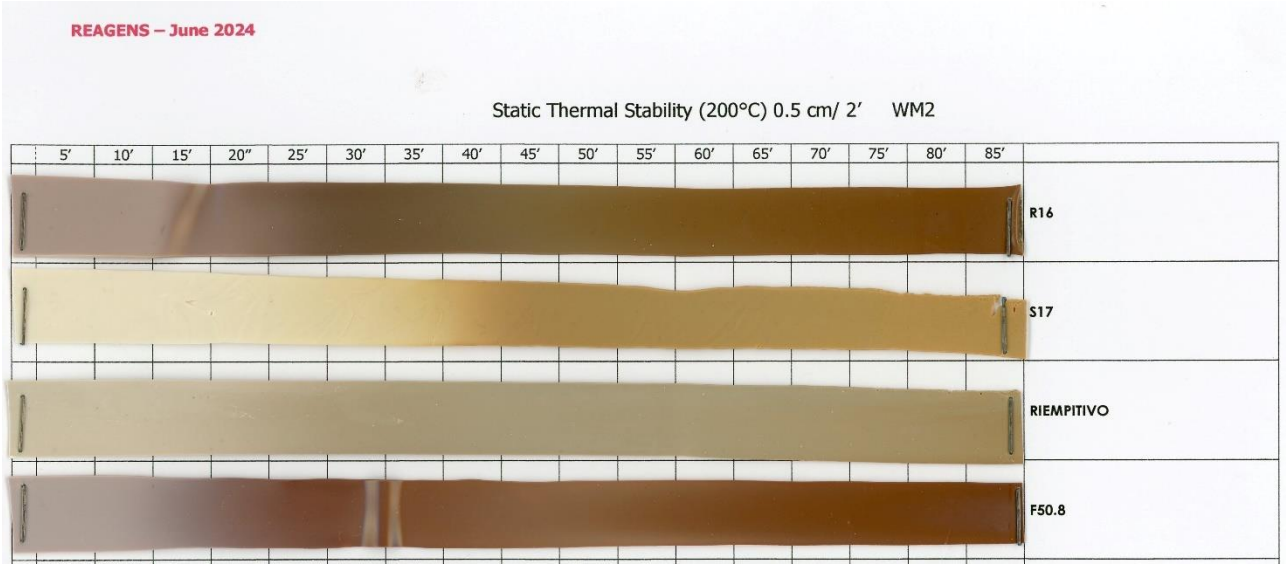

***Figure 4.4**: PVC compounds after colour retention analysis.*

This technique is aimed at evaluating colour retention at high temperatures. The PVC BEDDING displayed a good colour hold up to 20 minutes, and the S17 about 35 minutes.

4.2 FIRE BEHAVIOUR

4.2.1 Limiting Oxygen index (LOI)

The results obtained by LOI experiments are reported in Table 4.12.A and 4.12.B.

	R16	F50.8	R16_LSA	M16	PVC BEDDING	PVC BEDDING_LSA	BEDDING_G
Average (%O_2)	34	25	28	45	36	49	21
SD (%O_2)	+/1	+/1	+/1	+/1	+/1	+/1	+/1

***Table 4.12.A**: Results of LOI measurements.*

	G16	S17	G17
Average ($\%O_2$)	≤ 18	29	30
SD ($\%O_2$)	+/1	+/1	+/1

***Table 4.12.B**: Results of LOI measurements.*

The LOI, as discussed in the introduction, is a parameter used to assess the ease of extinction of a material. Starting with R16, the commercial PVC outer jacket used in FG16OR16, it demonstrates a LOI of 34%O_2. Based on its formulation (Table 4.1), the experimentally obtained LOI value aligns with expectations. A compound containing 50 phr of phthalic plasticizer typically starts with an LOI of around 24%O_2, as shown in Table 2.2. The presence of various flame retardants in the formulation boosts this value. MDH acts through a physical flame-retardant mechanism. As it releases its water of crystallization, it absorbs heat, dilutes the flame, and forms a protective layer of magnesium oxide. ATO, on the other hand, functions in the gas phase. During PVC combustion, ATO reacts with HCl, producing gaseous $SbCl_3$, which captures OH• and H• radicals that poison the flame. Additionally, the formulation includes 15 phr of chloroparaffin, which further enhances the LOI by enriching the gas phase with chlorine during combustion, providing added flame retardancy. In comparison, the two low smoke acidity PVC formulations for outer jackets, F50.8 and R16_LSA, show much lower LOI values, being 25%O_2 and 28%O_2, respectively. This is due to the incorporation of potent acid scavengers in the formulation to obtain lower values of smoke acidity during EN-60754-2 [3], as required by EN 13501-6 [29]. The reduced flame resistance in F50.8 can be attributed to the mechanism by which it achieves its low smoke acidity, indeed, F50.8 incorporates UPPCC and MDH, which act as strong acid scavengers in the gas phase, reacting with the HCl released during the decomposition of PVC, hence reducing the concentration of HCl in the gas phase. [42,43] However, without HCl, there is no synergic effect with ATO, therefore no flame poisoning. In contrast, the halogen-free outer jacket M16 in FG16OM16 achieves the highest LOI of 45%O_2, reflecting a strategy where the outer layer is the main defence against fire. In terms of bedding materials, PVC BEDDING and PVC BEDDING_LSA

exhibit LOI values of 36%O_2 and 49%O_2. The high LOI value of the PVC BEDDING is largely due to the combined effect of flame retardants and the significant presence of inorganic components (formulation in Table 4.1) like calcium carbonate, magnesium carbonate, and MDH. Magnesium carbonate, though less potent than MDH, still contributes to flame retardancy by breaking down at high temperatures, where it forms magnesium oxide, creating a protective barrier, and releases CO_2, which helps diluting the flame. Additionally, the formulation contains both ATO and zinc borate. In general, PVC beddings registered LOI significantly higher than the halogen-free BEDDING_G, which has an LOI of 21%O_2. This underscores the functionality of PVC-based beddings in enhancing the reaction- to-fire of cable system, particularly in comparison to their halogen-free counterparts. In fact, not only it reduces the heat release and the flame spread (FS), but also prevents the flaming dripping of non-flame retarded G16, which usually slides over the bedding (due to its incompatibility) and generates flaming droplets. In fact, the G16 insulation, used in both the FG16OR16 and FG16OM16 cables, shows a much lower LOI (≤18%O_2). Both the insulations, PVC-based and HF-based, used to make the FS17 and FG17 cables show a similar response to LOI analysis, measuring 29%O_2 and 30%O_2, respectively. The value of S17 is coherent with a formulation containing 46 phr of phthalic plasticizer and only 3 phr of ATO as FR.

4.2.2 MCC

The parameters obtained through MCC measurements are reported and explained in Table 4.13.

Parameter	Acronim	Unit	Description
Fire Growth Capacity	***FGC***	$\frac{J}{g * °C}$	It is defined as a measure considering chemical processes responsible for igniting and burning combustible materials (ignitability and flame spread).

			It is derived from other MCC measure measures such as ηc, ignition and burning temperatures.
Heat release capacity	η_c	$\frac{J}{g * °C}$	It is the maximum rate of heat release divided by the heating rate
Maximum specific heat release rate	Q_{max}	$\frac{J}{g}$	Maximum HRR obtained from the maximum oxygen consumed during the burning process
Peak Heat release temperature	T_{max}	°C	Temperature corresponding to the maximum heat release rate
Specific (total) Heat Release	h_c	$\frac{J}{g}$	It is derived from from the specific HRR(T) integral and represent the total heat released in the test
Yield of pyrolysis residue	Y_p	$\frac{g}{g}$	The initial and final weight ratios
Specific heat of combustion of fuel gases	$h_{c,gas}$	$\frac{J}{g}$	It is the heat of combustion per gram of fuel burned in the combustor and accounts for the energy released from the combustion of the fuels in the gas phase

***Table 4.13**: summary of MCC parameters.*

A summary of the averages, along with their corresponding standard deviations, of the results obtained by MCC measurements is reported in Table 4.14.A and 4.14.B and 4.14.C.

	R16	F50.8	R16_LSA	M16
***FGC* (J/g·°C)**	96,51 ± 1,99	105,54 ± 3,96	76,22 ± 2,40	281,57 ± 4,63
η_c (J/g·°C)	283,80 ± 14,72	261,15 ± 13,72	227,44 ± 9,49	417,06 ± 18,42
Q_{max} (J/g)	166,83 ± 9,41 (Stage 1) 47,58 ± 1,46 (Stage 2)	168,08 ± 9,36 (Stage 1) 46,65 ± 2,83 (Stage 2)	103,84 ± 3,66 (Stage 1) 19,82 ± 2,73 (Stage 2) 30,84 ± 2,97 (Stage 3)	374,41 ± 11,56
T_{max} (°C)	308,8 ± 1,2 (Stage 1) 469,7± 0,3 (Stage 2)	330,6 ± 1,2 (Stage 1) 469,2 ± 0,8 (Stage 2)	301,2 ± 2,9 (Stage 1) 374,0 ± 3,1 (Stage 2) 463,1 ± 4,1 (Stage 3)	496,6 ± 0,4
h_c (J/g)	12,26 ± 0,48	13,51 ± 0,59	8,65 ± 0,55	16,59 ± 0,19
Y_p (g/g)	18,59 ± 0,72	25,36 ± 1,04	16,70 ± 0,95	31,47 ± 0,31
$h_{c,gas}$ (J/g)	96,51 ± 1,99	105,54 ± 3,96	76,22 ± 2,40	281,57 ± 4,63

***Table 4.14.A**: summary of the averages and st. dev. derived from results of MCC tests on R16, F50.8; R16_LSA and M16.*

	BEDDDING	BEDDING_LSA	BEDDING_G	G16
***FGC* (J/g·°C)**	51,80 ± 0,62	40,36 ± 0,47	97,71 ± 0,64	1094,66 ± 63,45
η_c (J/g·°C)	168,81 ± 11,39	156,42 ± 3,79	232,28 ± 21,56	1543,82 ± 187,36

Q_{max} (J/g)	123,32 ± 9,16 (Stage 1) 26,76 ± 1,12 (Stage 2)	96,11 ± 5,92 (Stage 1) 37,43 ± 0,85 (Stage 2)	168,80 ± 4,43	1352,52 ± 145,27
T_{max} (°C)	321,0 ± 1,0 (Stage 1) 464,2 ± 2,8 (Stage 2)	310,9 ± 1,8 (Stage 1) 480,8 ± 1,4 (Stage 2)	490,8 ± 0,5	499,1 ± 1,2
h_c (J/g)	6,29 ± 0,44	5,36 ± 0,08	10,27 ± 0,11	49,75 ± 1,79
Y_p (g/g)	11,30 ± 0,70	10,56 ± 0,16	45,62 ± 0,72	52,89 ± 3,22
$h_{c,gas}$ (J/g)	51,80 ± 0,62	40,36 ± 0,47	97,71 ± 0,64	1094,66 ± 63,45

***Table 4.14.B**: summary of the averages and st. dev. derived from results of MCC tests on PVC and HF based baddings and G16.*

	S17	**G17**	**G16**
***FGC* (J/g·°C)**	115,32 ± 0,58	231,43 ± 18,56	1094,66 ± 63,45
η_c (J/g·°C)	380,33 ± 10,54	370,39 ± 11,66	1543,82 ± 187,36
Q_{max} (J/g)	262,89 ± 16,70 (Stage 1) 45,36 ± 0,60 (Stage 2)	400,82 ± 10,99	1352,52 ± 145,27
T_{max} (°C)	319,1 ± 1,0 (Stage 1) 465,0 ± 0,2 (Stage 2)	491,1 ± 1,5	499,1 ± 1,2
h_c (J/g)	13,70 ± 0,05	18,67 ± 0,55	49,75 ± 1,79
Y_p (g/g)	19,57 ± 0,09	33,06 ± 1,10	52,89 ± 3,22

$h_{c,gas}$ **(J/g)**	115,32 ± 0,58	231,43 ± 18,56	1094,66 ± 63,45

Table 4.14.C*: summary of the averages and st. dev. derived from results of MCC tests on S17 and G17.*

The values of Q_{max} (J/g) and h_c (J/g) are two important parameters derived from HRR curves, representing the maximum peak and the integral of the curve, respectively. R16 exhibits an h_c of 12.26 J/g, and the Q_{max} is 166.83 J/g. In contrast, M16 displays a significantly higher h_c of 16.59 J/g and a sharp increase in Q_{max} to 374.41 J/g. F50.8 shows a similar h_c of 13.51 J/g and a Q_{max} of 168.08 J/g to R16. R16_LSA shows the lowest parameters among outer jackets, with a h_c at 8.65 J/g and a Q_{max} of 103.84 J/g. The bedding materials show similar trends. Standard PVC BEDDING has an h_c of 6.29 J/g and a Q_{max} of 123.32 J/g, while BEDDING_LSA has a lower h_c at 5.36 J/g and a reduced Q_{max} of 96.11 J/g, and instead BEDDING_G exhibits a higher h_c of 10.27 J/g and a Qmax of 168.80 J/g, mirroring the general trend of HF materials.

Fire performance can be estimated by examining both FGC and η_c, which together help further corroborate the trends established by Q_{max} and h_c. FGC, which is derived from other MCC measure parameters such as η_c, ignition and burning temperatures, is considered a relevant index regarding ignitability and flame spread. η_c, is a variable that correlates flammability to material properties. It is known to be a good predictor of flammability and shows the tendency of a material to ignite [43]. R16, the PVC based outer jacket used in FG16OR16, has an FGC of 96.51 J/g·K and an η_c of 283.80 J/g·K. In contrast, M16, the HF compound used as outer jacket in FG16OM16, displays a much higher FGC of 281.57 J/g·K and η_c of 417.06 J/g·K. F50.8 and R16_LSA, LSA PVC based formulations, behave differently. While F50.8 exhibits an FGC slightly higher at 105.54 J/g·K, and a lower η_c of 261.15 J/g·K, offering performances similar to R16; R16_LSA shows the lowest FGC among outer jacket compounds at 76.22 J/g·K and a reduced η_c of 227.44 J/g·K, indicating that this compound performs better in terms of reaction- to-fire. When looking at the bedding materials, the standard PVC bedding shows a low FGC of 51.80 J/g·K and a η_c of 168.81 J/g·K, indicating good fire performance. The BEDDING_LSA variant further reduces these values, with an FGC of 40.36 J/g·K and an η_c of 156.42 J/g·K,

reinforcing that LSA formulations can maintain, or even improve, fire safety, which is reflected by the higher fire safety class of B_{2ca} obtained by the FG16OR16 LSA geometry developed by PVC4cables. On the other hand, the HF BEDDING_G exhibits a higher FGC of 97.71 J/g·K and η_c of 232.28 J/g·K, reflecting the trend seen in other HF materials: a tendency in contributing to fire growth more easily and release more heat compared to PVC based beddings.

Another key parameter derived from MCC measurements is the specific heat of combustion of fuel gases ($h_{c,gas}$). An interesting correlation can be observed between h_c and $h_{c,gas}$, specifically the percentage variation between these two values. When comparing PVC and HF based compounds, a clear distinction emerges, reflecting different strategies used to enhance fire performance through FRs. For PVC based compounds the $\Delta h_c \rightarrow h_{c,gas}$ was of 687% for R16, of 723% for the PVC commercial bedding and of 742% for S17. Instead, the HF formulations showed much higher percentages: 1597% for M16, 851% for BEDDING_G and 1140% for G17. The significantly higher $\Delta h_c \rightarrow h_{c,gas}$ (%) for HF compounds than the one registered for PVC based formulations, particularly in the case of M16, suggests the use of FRs that operate in the gas phase, likely through mechanisms such as fuel dilution. LSA formulations showed similar results to standard PVC compounds, exhibiting $\Delta h_c \rightarrow h_{c,gas}$ was of 681% for F50.8, 781% for R16_LSA and 653% for BEDDING_LSA.

The specific HRR curves registered during MCC measurements are reported in Figure 4.5, Figure 4.6 and Figure 4.7 (outer jackets, beddings and insulations, respectively).

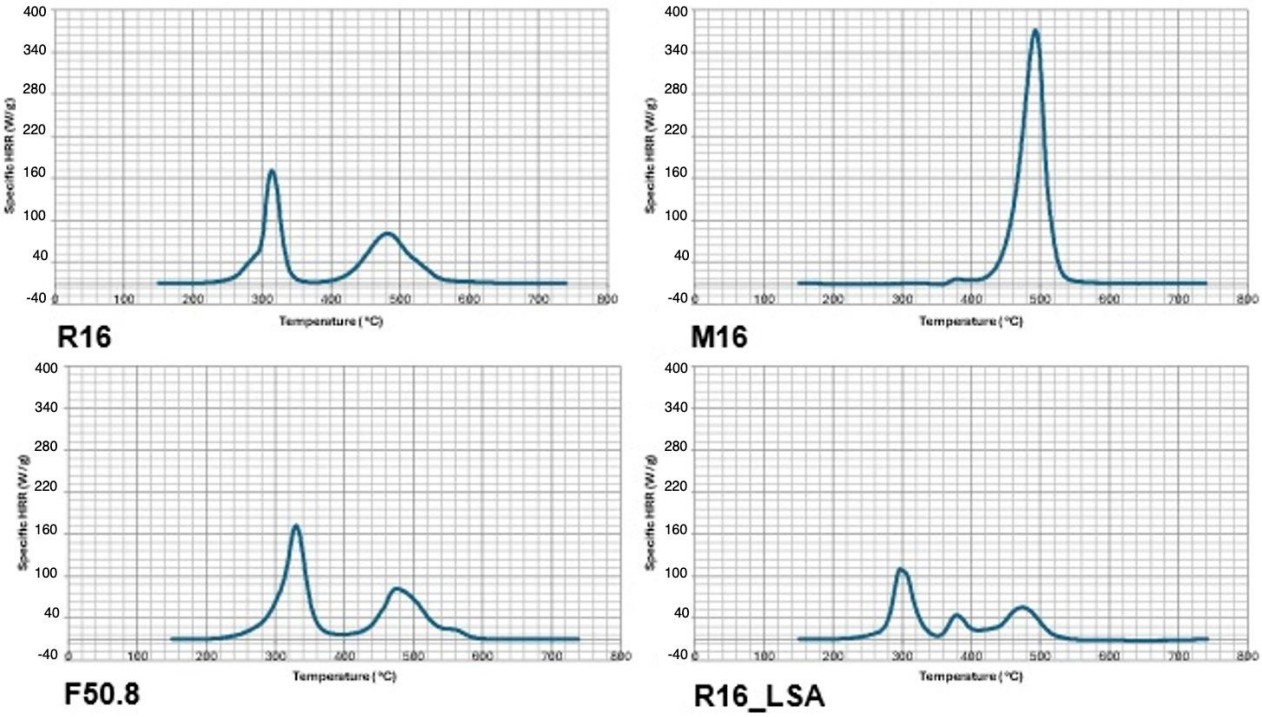

***Figure 4.5**: HRR curves of compounds used as outer jackets in the manufacturing of cables with FG16OR16 or FG16OM16 geometries.*

When comparing the HRR curves of the compounds used for outer jackets in cables with FG16OR16 or FG16OM16 geometries, distinct patterns emerge. The typical pattern manifested by plasticized PVC formulations presents two peaks at distinct stages: the first and highest one is related to the oxygen consumption from the combustion of fuels released by the thermal dehydrochlorination of PVC resins which occurs between 220 °C and 350°C. The second peak starts at temperatures above 450 °C and is related to the volatile fuels release by the breakdown of the condensation products from the first stage, mainly aliphatic hydrocarbons. R16 and F50.8 exhibits this behavior. The commercial R16 exhibits two peaks: the first, higher peak occurs at 308.8 ± 1.21°C, during this step the major emission product is HCl, resultant from the thermal decomposition of PVC itself. Organic substances like DINP and lubricants volatilize and combust. On the contrary, MDH release water vapor as it decomposes, which absorbs heat and reduces fuel concentration. The second, much broader second peak is around 500°C and is related to the combustion of unsubstituted aromatics and alkyl aliphatic moieties from the first stage. F50.8 shows a similar pattern, with the first peak slightly shifted to a higher temperature (T_{max} = 330.6 ± 1.22°C). In contrast, R16_LSA presents three peaks, with the highest

occurring at 301.2 ± 2.93°C, a lower middle peak, and a broader third peak. The HF M16 exhibits a completely different behaviour, with only a single, higher and narrow peak at 496.62 ± 0.41°C.

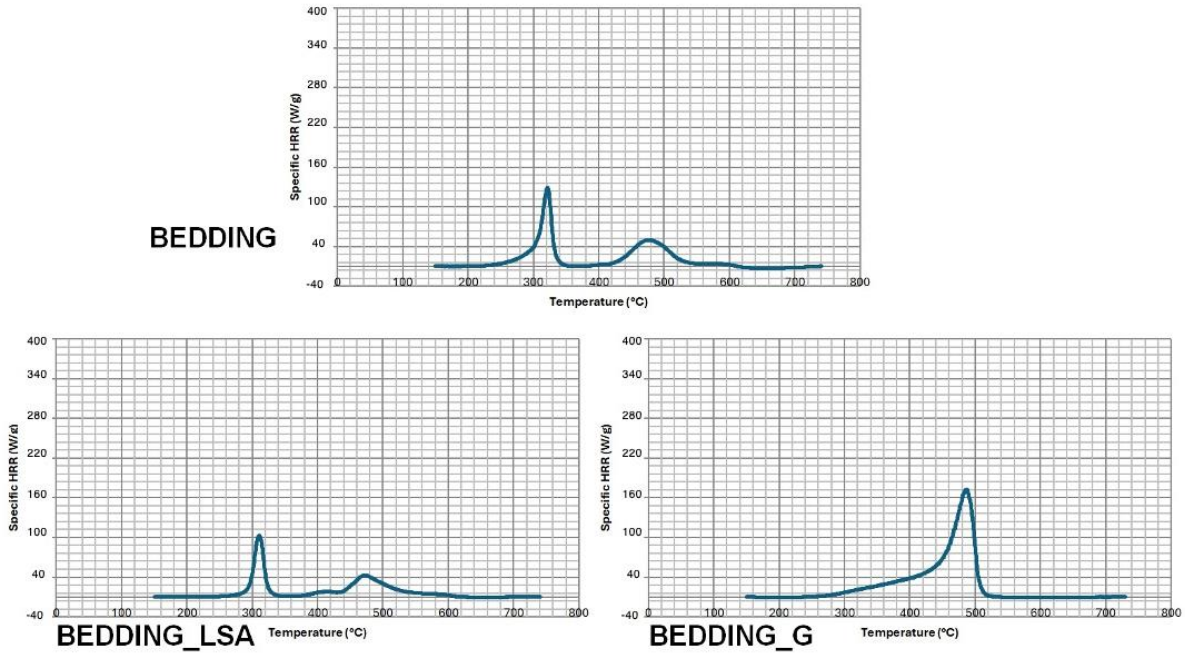

***Figure 4.6**: HRR curves of compounds used as beddings in the manufacturing of cables with FG16OR16 or FG16OM16 geometries.*

The commercial PVC bedding displays an HRR profile typical of PVC-P, with the first peak occurring at 321.0 ± 0.96°C. BEDDING_LSA followed a similar pattern but with lower peaks. In contrast, the HF BEDDING_G exhibits only one very high and broad peak at 490.8 ± 0.54°C, with the HRR starting to increase near 300°C.

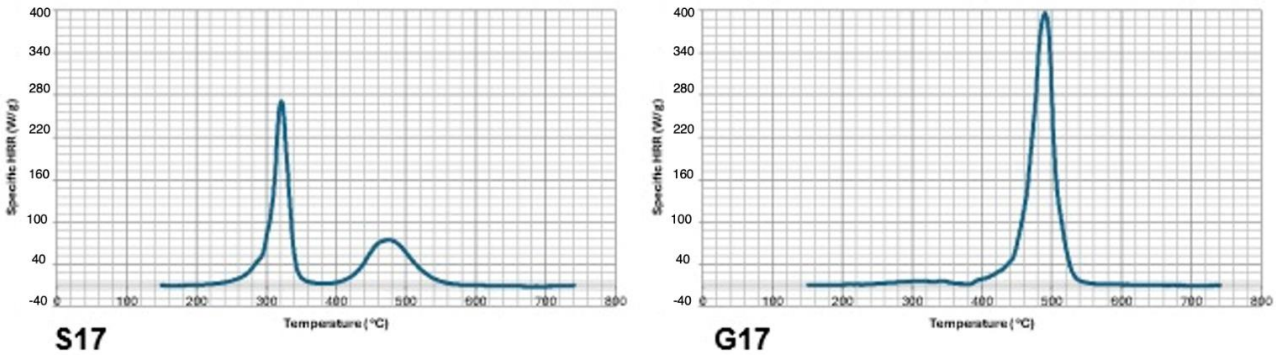

***Figure 4.7**: HRR curves of compounds used as insulations in the manufacturing of cables with S17 (left) and G17 (right) geometries.*

The comparison between the HRR curves of the S17 and G17 insulations reflects the established trend for PVC based and HF based compounds. S17 shows the typical PVC-P pattern, with the first, higher and narrower peak occurring at 319.1 ± 0.97°C. In contrast, G17 exhibits a single, very high peak at 491.1 ± 1.49°C, aligning with the general behaviour manifested by HF compounds.

4.2.3 Cone Calorimetry

Cone calorimetry tests were performed at two incident heat fluxes, the first one at 35 kW/m², corresponding to a temperature of 670 °C, to mimic a scenario of near-flashover and the second one at 62 kW/m², resulting in a temperature of 825 °C to recreate post-flashover conditions.

Table 4.15 presents the parameters derived from heat release rate (HRR) and smoke production rate (SPR) curves and their meaning.

PARAMETER	ACRONIM	UNIT	DESCRIPTION
Time To Ignition	TTI	s	Time from the start of the test to the ignition
Time to Flame Out	TFO	s	Time from the start of the test until the flame completely extinguishes
Time To Peak	TTP	s	Time corresponding to the maximum of the HRR curve
Fire Growth Rate Index	FIGRA	W/s	Index of fire growth obtained from the HRR curve following the eq. (2) reported in 6.3.3
Total Heat Release	THR	MJ/m^2	Total heat released during the measurement
Peak of Heat Release Rate curve	pHRR	kW/m^2	Maximum value of the HRR curve
Total Smoke Production	TSP	m^2	Total smoke produced during the analysis

Peak of Smoke Production Rate curve	pSPR	m^2/s	Maximum value of the SPR curve
Weight Loss	WL	%	Variation in weight measured during the analysis expressed as percentage

***Table 4.15**: summary of Cone Calorimetry parameters.*

A summary of the averages and standard deviations of the results obtained through cone calorimetry measurement is reported in Table 4.16.A and 4.16.B (35kW/m²) and Table 4.17.B and 4.17.B (62kW/m²).

35kW/m²	**TTI (s)**	**TFO (s)**	**TTP (s)**	**pHRR (kW/m^2)**	**THR (MJ/m^2)**	**$FIGRA_{0,2MJ}$ (W/s)**
R16	23 ± 1	140 ± 0	66 ± 0	172 ± 3,2	18,8 ± 1,4	2481 ± 47
M16	114 ± 11	471 ± 13	273 ± 34	163,5 ± 5,6	30,9 ± 0,3	587 ± 82
F50.8	27 ± 3	219 ± 8	62 ± 2	251 ± 10,8	22 ± 0,6	4072 ± 111
R16_LSA	32 ± 5	157 ± 7	58 ± 8	176 ± 11,2	17,7 ± 1	2822 ± 96
BEDDDING	30 ± 1	137 ± 3	65 ± 2	145,3 ± 6,4	13,8 ± 0,5	2101 ± 298
BEDDING_G	37 ± 0	226 ± 6	84 ± 4	214 ± 18,9	18,6 ± 1,4	2371 ± 108
BEDDING_LSA	42 ± 3	76 ± 5	68 ± 2	71,5 ± 8,1	9,8 ± 0,7	687 ± 36
S17	23 ± 1	178 ± 16	65 ± 6	172 ± 13,6	20,2 ± 0,1	2557 ± 134
G17	55 ± 7	233 ± 4	146 ± 2	189,3 ± 2,9	22,5 ± 0	1307 ± 84
G16	41 ± 4	280 ± 16	89 ± 2	427,2 ± 23,7	39,2 ± 1,2	4620 ± 223

***Table 4.16.A**: Results of cone calorimetry analysis conducted at a specific heat flux of 35 kW/m².*

35kW/m²	SMOGRA (m^2/s^2)	Weight loss (%)	TSP (m^2)	pSPR (m^2/s)
R16	/	77,2 ± 7,6	4,8 ± 0,1	0,062 ± 0,002
M16	/	53,2 ± 1,3	2,1 ± 0	0,031 ± 0,001
F50.8	/	60,5 ± 0,2	4,7 ± 0,1	0,069 ± 0,002
R16_LSA	/	48,5 ± 2,1	1,9 ± 0,2	0,031 ± 0,004
BEDDDING	/	49,3 ± 0,5	2,9 ± 0,2	0,046 ± 0,009
BEDDING_G	/	26,1 ± 0,2	1,3 ± 0,1	0,026 ± 0,002
BEDDING_LSA	/	51,9 ± 0,7	1,5 ± 0,3	0,024 ± 0,004
S17	/	74,9 ± 2,6	7,6 ± 0,2	0,116 ± 0
G17	/	55 ± 2,9	1,6 ± 0,2	0,023 ± 0,002
G16	/	102,2 ± 4,2	2,8 ± 0,3	0,037 ± 0,003

***Table 4.16.B**: Results of cone calorimetry analysis conducted at a specific heat flux of 35 kW/m².*

62kW/m²	TTI (s)	TFO (s)	TTP (s)	pHRR (kW/m^2)	THR (MJ/m^2)	$FIGRA_{0,2MJ}$ (W/s)
R16	10 ± 0	168 ± 8	35 ± 2	189,6 ± 11,2	22,8 ± 0,6	4538 ± 241
M16	41 ± 3	388 ± 34	175 ± 29	211,4 ± 24,7	34,2 ± 3	1641 ± 127

F50.8	9 ± 4	204 ± 14	36 ± 3	318,2 ± 38	23,9 ± 2,2	8512 ± 2058
R16_LSA	11 ± 2	178 ± 13	42 ± 9	218 ± 30	20,3 ± 1,8	5411 ± 614
BEDDING	11 ± 2	196 ± 34	41 ± 2	166,5 ± 8,6	15,6 ± 2,2	3772 ± 418
BEDDING_G	17 ± 2	210 ± 5	57 ± 0	313,4 ± 8,1	22,4 ± 0,7	5334 ± 168
BEDDING_LSA	86 ± 9	113 ± 8	102 ± 5	93,7 ± 58,8	11,6 ± 1,9	1325 ± 824
S17	10 ± 3	190 ± 38	45 ± 13	211,9 ± 9,5	24,9 ± 5,1	5435 ± 764
G17	21 ± 1	370 ± 7	83 ± 11	241,2 ± 8,2	29,1 ± 3,5	3656 ± 219
G16	18 ± 1	296 ± 77	51 ± 4	563,6 ± 63,1	39,2 ± 0,4	9223 ± 1152

***Table 4.17.A**: results of cone calorimetry analysis conducted at a specific heat flux of 62 kW/ m².*

62kW/m²	**SMOGRA (m^2/s^2)**	**Weight loss (%)**	**TSP ($m^{2)}$**	**pSPR (m^2/s)**
R16	/	77,0 ± 0,3	6,9 ± 0,2	0,111 ± 0,001
M16	/	60,1 ± 1,6	3,1 ± 0,4	0,043 ± 0,003
F50.8	/	69,3 ± 4,7	5,8 ± 0,1	0,109 ± 0,011
R16_LSA	/	53,1 ± 0,6	2,9 ± 0,2	0,052 ± 0,005
BEDDING	/	55,7 ± 3,5	2,7 ± 0,2	0,066 ± 0,005
BEDDING_G	/	29,5 ± 1	1,6 ± 0	0,042 ± 0,004

BEDDING_LSA	/	61,2 ± 4,9	1,2 ± 0,3	0,042 ± 0,005
S17	16 ± 1	78,1 ± 3,5	9,4 ± 1,4	0,151 ± 0,002
G17	/	61,7 ± 0,2	1,8 ± 0	0,037 ± 0,002
G16	/	100,1 ± 2,6	3,5 ± 0,3	0,062 ± 0,002

***Table 4.17.B**: results of cone calorimetry analysis conducted at a specific heat flux of 62 kW/ m².*

4.2.3.1 Results

The average of the results for each sample regarding TTI, TFO and TTP are presented in Figure 4.8 and 4.9, corresponding to 35 kW/m²and 62 kW/m² respectively.

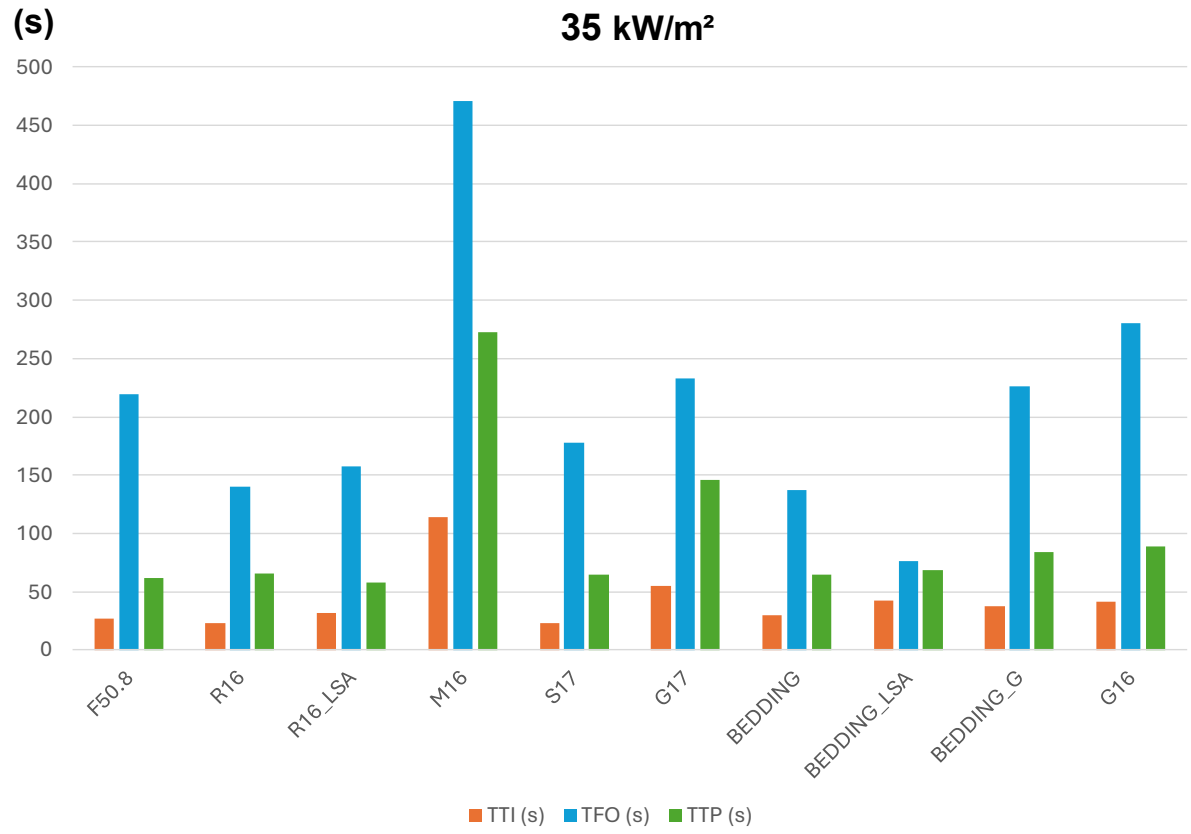

***Figure 4.8**: TTI vs TFO vs TTP (35 kW/m²)*

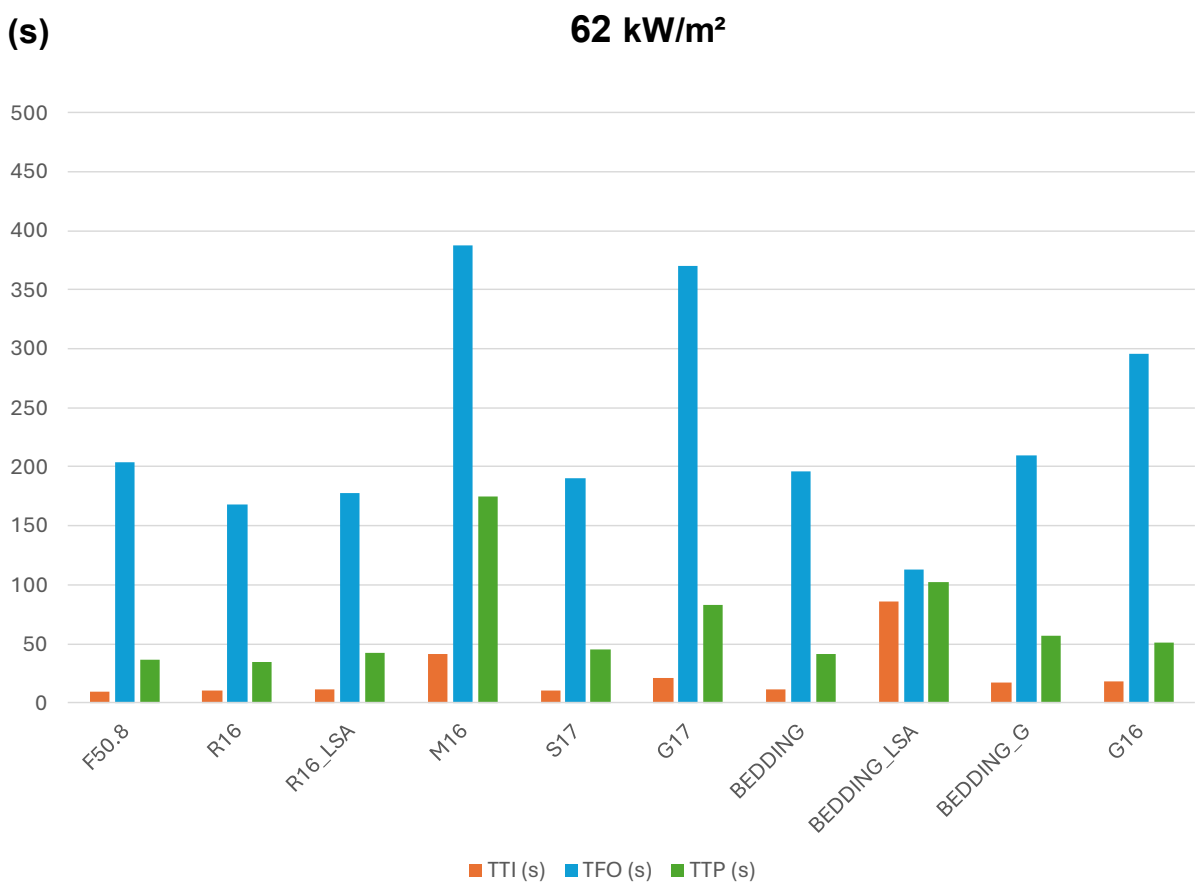

***Figure 4.9**: TTI vs TFO vs TTP (62 kW/m²)*

Among the times recorded during the cone calorimetry tests, TTP is the one to give more information as it expresses the time it took to reach the peak of the HRR curve. At 35 kW/m², R16 showed a TTP of 66 ± 0 s, while M16 displayed the highest TTI among all compounds (273 ± 34). The LSA PVC formulations (F50.8 and R16_LSA) for outer jackets registered similar values to the commercial R16. For the bedding materials, the PVC bedding and its HF counterpart demonstrated comparable TTP, with the one of BEDDING_G being only slightly higher. BEDDING_LSA recorded a value of TTP similar to the one of the commercial PVC bedding. G17 exhibited higher TTP than S17 at 35 kW/m².

At 62 kW/m², the value of TTP for R16 decreased to 35 ± 2 s, the TTP of M16, while remaining higher than the one of R16, suffered a substantial decrease to 175 ± 29 s. F50.8 and R16_LSA continued to record similar values to the commercial R16. The

difference in TTP between the PVC bedding and its HF counterpart decrease, as the BEDDING_G value of TTP was 57 ± 0. Notably, BEDDING_LSA showed an increase in TTP at higher incident heat fluxes. At 62 kW/m², the TTP of G17 dropped, narrowing the gap with S17.

The averages of the results of FIGRA are reported in Figure 4.10.

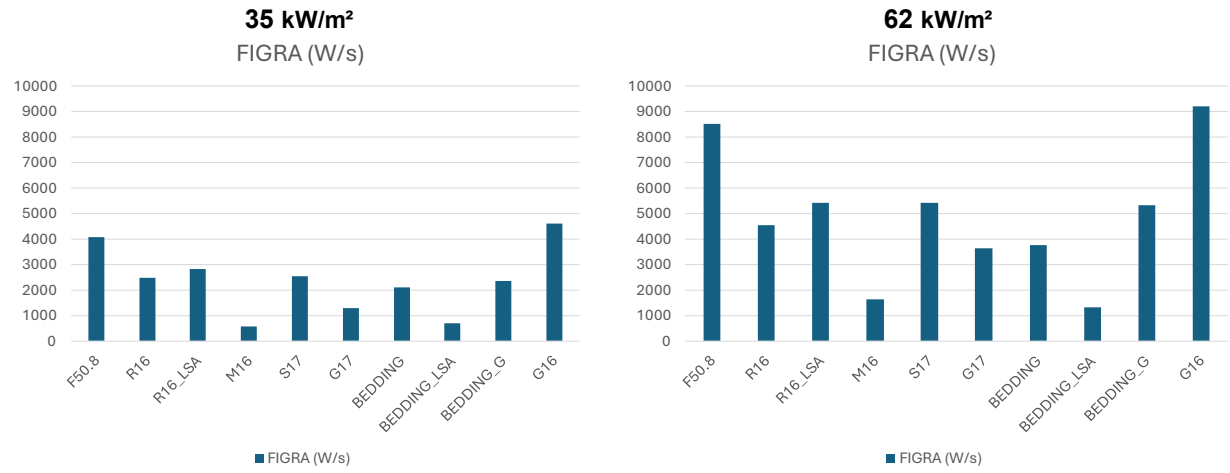

***Figure 4.10**: FIGRA results.*

At 35 kW/m² R16 showed a value of FIGRA of 2481 ± 47 W/s, while M16 registered a much lower value (587 ± 82 W/s). The R16_LSA formulation showed results similar to R16, while F50.8 demonstrated a higher FIGRA. Conversely, HF bedding exhibited higher FIGRA values compared to the PVC-based bedding, while BEDDING_LSA exhibited significantly lower FIGRA. S17 showed only slightly higher FIGRA values compared to G17.

At 62 kW/m², the registered FIGRA of R16 rose to 4538 ± 241 W/s and the one of M16 to 1641 ± 127 W/s. R16_LSA showed an increase in FIGRA comparable to the one of commercial R16, while F50.8 demonstrated a noticeably higher FIGRA of 8512 ± 2058 W/s. This decline in performance can be attributed to the role of UPPCC and MDH, which remove HCl released from PVC resin during its decomposition, thereby as mentioned before, without HCl, there is no synergic effect with ATO, therefore no flame poisoning.

The PVC bedding suffered an increase in FIGRA to 3772 ± 418 W/s, but the decrease in fire resistance of BEDDING_G was more pronounced, registering a FIGRA of 5334 ± 168 W/s. Notably, BEDDING_LSA exhibited significantly lower FIGRA (1325 ± 824 W/s) values than the commercial PVC bedding at 62 kW/m². The internal G16 insulation, common to both FG16OR16 and FG16OM16, performs poorly in terms of FIGRA at both heat fluxes, with significantly higher values compared to the outer layers. Lastly, both S17 and G17 insulations recorded an increase in FIGRA to 5435 ± 764 W/s and 3656 ± 219 W/s, respectively.

The averages of the results of pHRR are reported in Figure 4.11.

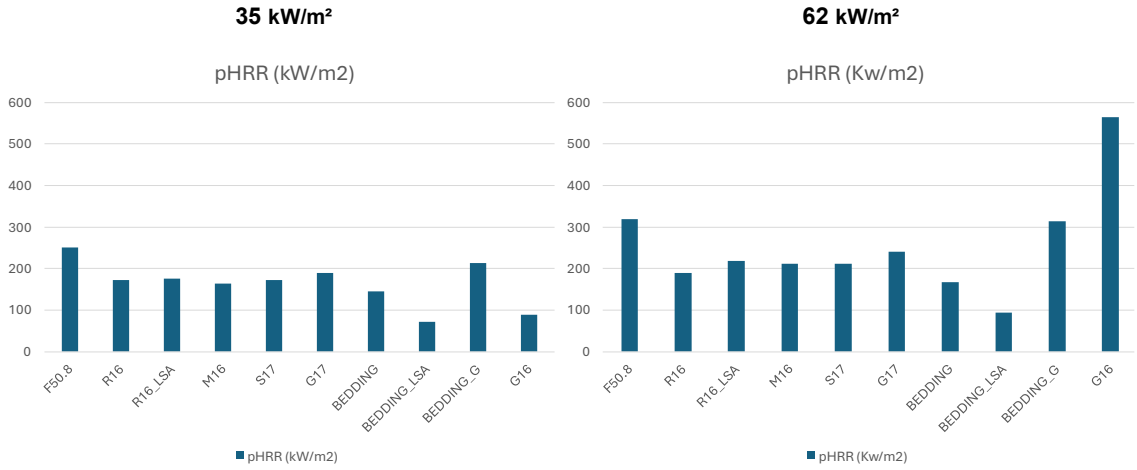

***Figure 4.11**: pHRR results.*

The value of pHRR for R16, the commercial PVC outer jacket, measured at 35 kW/m² is similar to the pHRR of the curve recorded at 62 kW/m², maintaining values around 200 kW/m². M16, the HF option, remains constant across both heat fluxes, with pHRR values also near 200 kW/m². Relating to the PVC LSA alternatives for outer jackets, R16_LSA is comparable to R16, but F50.8 performs worse, with higher pHRR values, particularly at 62 kW/m². The PVC bedding shows no significant increase in pHRR at 62 kW/m², with BEDDING_LSA following a similar trend but maintaining lower pHRR values overall. In contrast, the pHRR for HF BEDDING_G rises sharply at higher fluxes. S17 and G17 exhibit comparable results, though S17 has slightly lower pHRR values, with this difference becoming more pronounced at 62 kW/m².

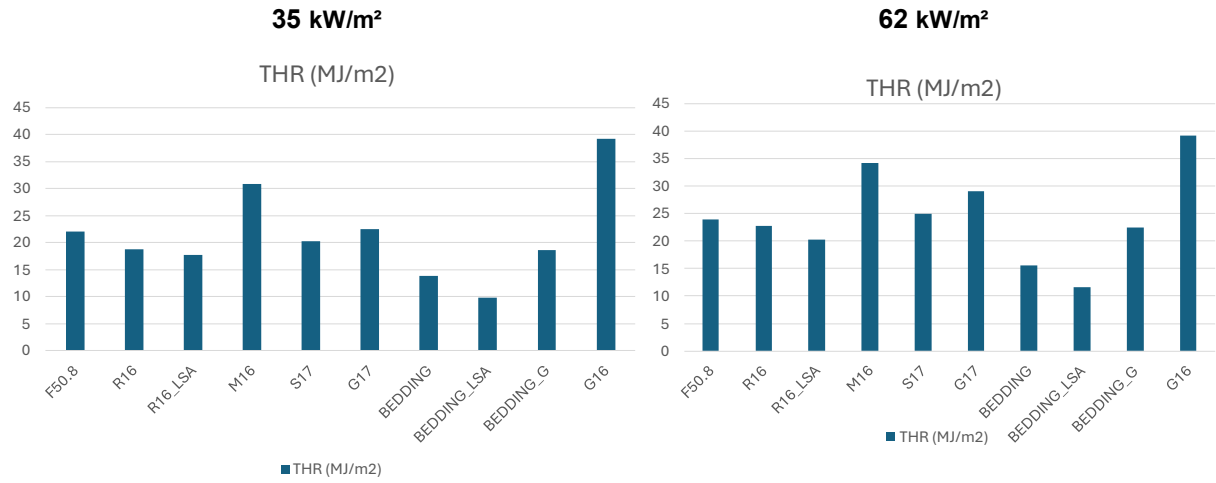

***Figure 4.12**: THR results.*

Figure 4.13 above illustrate the THR in MJ/m² for the cable components tested at heat fluxes of 35 kW/m² and 62 kW/m². The THR values reflects the overall heat released by the materials during combustion, an important parameter in assessing the fire performance of compounds.

At 35 kW/m², the PVC based compound R16, used in the jacket of FG16OR16, exhibits a lower THR (22,8 ± 0,6 MJ/m²) compared to its HFFR counterpart M16 (34,2 ± 3 MJ/m²) in FG16OM16. While M16 performs well in delaying the TTP, it releases a substantial amount of heat once ignited, whereas R16 demonstrates PVC's capacity to limit total heat release during combustion. The R16_LSA formulation performed comparably to R16 in terms of THR, however, F50.8 showed slightly higher values than the commercial PVC outer jacket. This behavior is similarly observed in the beddings, with the HF BEDDING_G showing higher THR values than the PVC based bedding, while the Bedding_LSA exhibited a lower THR compared to the commercial PVC bedding. At 35 kW/m², G17 displayed slightly higher THR values compared to S17.

At 62 kW/m², R16 and PVC bedding maintained stable THR values, showing little performance loss despite the higher incident heat flux. In contrast, M16 continued to exhibit an higher THR, while R16_LSA continued to perform similarly to R16 and also F50.8 recorded similar values. BEDDING_G further widened the gap with the PVC beddings. The increased heat flux amplified the differences between HF rubbers and

PVC based materials, with HF compounds showing a more pronounced rise in THR. BEDDDING_LSA maintained more moderate THR values even at 62 kW/m². The high THR from G16 inner insulation at both heat fluxes reinforces the strategy employed in the FG16OR16 and FG16OM16 cables, where reaction- to-fire is heavily reliant on the outer layers (jacket and bedding) to protect the cable, with no emphasis on the insulation material's ability to resist combustion. The difference in THR between G17 and S17 became more pronounced at 62 kW/m², where G17 experienced a more significant increase in THR, further widening the gap between the two materials under higher heat fluxes. This behavior supports the overall trend observed in all HF materials, where G17, like other HF compounds under analysis, tends to release more heat at elevated fluxes compared to PVC based counterparts.

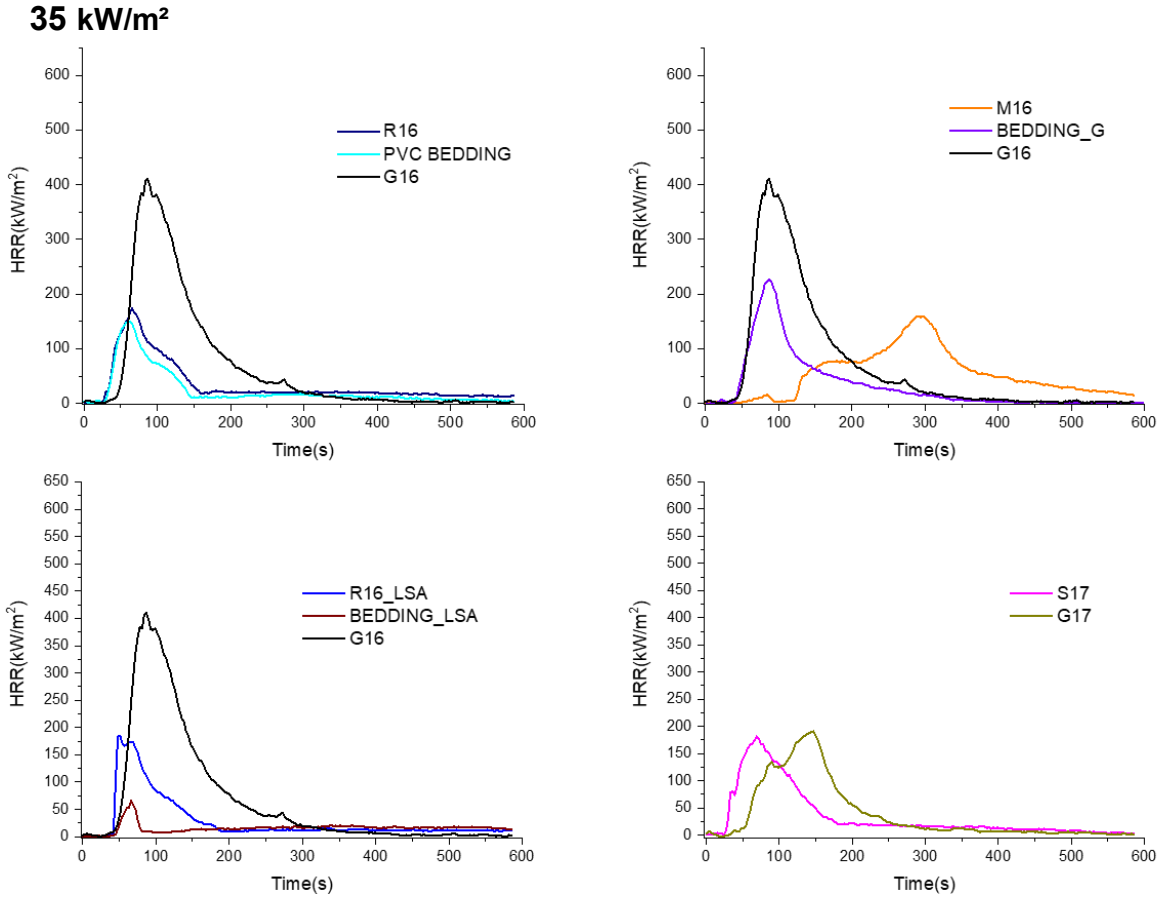

***Figure 4.13**: HRR curves at 35 kW/m² of: compounds of FG16OR16 (top left); compounds of FG16OM16 (top right); LSA alternatives for compounds of FG16OR16 (bottom left); compounds of FS17 and FG17 (bottom right).*

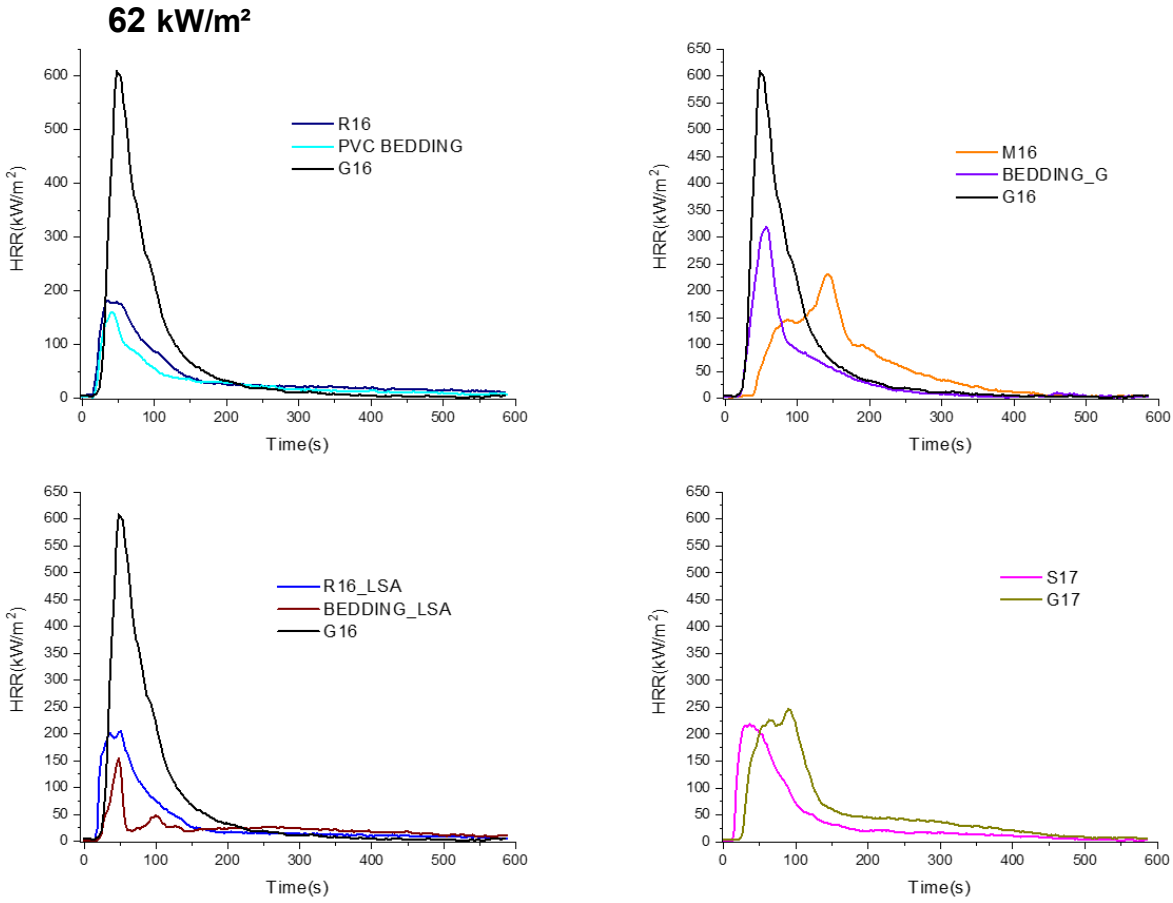

***Figure 4.14**: HRR curves at 62 kW/m² of: compounds of FG16OR16 (top left); compounds of FG16OM16 (top right); LSA alternatives for compounds of FG16OR16 (bottom left); compounds of FS17 and FG17 (bottom right).*

The graphs, reported in Figure 4.13 and Figure 4.14, above show the HRR curves, at 35 kW/m² and 62 kW/m², of compounds used in the manifacture of cables of FG16OR16, FG16OM16, FS17 and FG17 geometries: In the top left corner are represented the HRR curves of R16, the PVC bedding and G16 (FG16OR16); in the top right corner the HRR curves of M16, the HF bedding and G16 (FG16OM16); in the bottom left corner the HRR curves of R16_LSA, BEDDING_LSA and G16 (LSA version of FG16OR16); in the bottom right corner the HRR curves of S17 and G17 (FS17 vs FG17).

This representations aims to provide a comprehensive overview on the thermal behaviour of each compound within its own cable geometry at both incident heat fluxes, while at the same time have a clear comparison of the differences present among the compounds used to manifacture different cable geometries. For FG16OR16, the PVC bedding and R16 outer jacket demonstrated similar profiles at both incident heat fluxes, with only a slight increase in peak HRR at higher fluxes. In contrast, the HF alternatives exhibited higher and broader peaks, with the peak for the M16 compound notably shifted to later times, though this delay is significantly reduced at 62 kW/m². The LSA PVC formulations, particularly the bedding, showed narrower and lower peaks at both heat fluxes. The inner insulation G16 exhibited the poorest fire performance among all compounds at both heat fluxes. In FG16OR16, the R16 PVC outer jacket and PVC bedding each contribute to the cable's overall flame resistance. On the other hand, FG16OM16 relies more heavily on the outer M16 jacket as the primary barrier against fire, with the bedding playing a minor role in fire protection. At 35 kW/m², S17 and G17 showed similar profiles, with the G17 curve occurring at later times. However, this delay was notably reduced at 62 kW/m², following a pattern similar to that observed with M16.

Table 4.18 presents the values of ΔFIGRA (%) and ΔTHR (%).

Compound	**ΔFIGRA (%)** *62 kW/m² - 35 kW/m²*	**ΔTHR (%)** *62 kW/m² - 35 kW/m²*
F50.8	+ 108 %	+ 8,6 %
R16	+ 82,9 %	+ 21,3 %
R16_LSA	+ 91,7 %	+ 14,7 %
M16	+ 179,6 %	+10,7 %
S17	+ 112,5 %	+ 23,3 %
G17	+ 179,7 %	+ 29,3 %
BEDDING	+ 79,5 %	+ 13 %
BEDDING_LSA	+ 92,9 %	+ 18,4 %
BEDDING_G	+ 125 %	+ 20,4 %
G16	+ 99,6 %	+ 0 %

***Table 4.18**: ΔFIGRA and ΔTHR of the averages of cone calorimetry results, (62 kW/m² - 35 kW/m²).*

ΔTHR and ΔFIGRA values were calculated by subtracting the values of THR and FIGRA, respectively, registered at 35 kW/m² from the values recorded at 62 kW/m². The percentage variation was evaluated by dividing the ΔTHR and ΔFIGRA by the value obtained at 35 kW/m² and multiplying per 100 and indicated in Table 4.17. These values put emphasis on the proportional loss of reaction-to-fire for each compound when exposed at higher incident heat fluxes.

The PVC outer jacket of R16 quality and its LSA alternative, R16_LSA, exhibit ΔFIGRA (%)values of +82,9% (+2057 W/s) and +91,7% (+2589 W/s), respectively. The corresponding ΔTHR (%) increases were +21,3% (+4 MJ/m²) and +14,7% (+2.6 MJ/m²), respectively. In contrast, the M16 compound shows an increase in FIGRA (+1054 W/s) not as large as that of other compounds, however, the percentage variation (+179,6%) is noteworthy. This indicates that, although M16 performs well at lower heat flux levels, its ability to resist fire growth diminishes more drastically as the heat flux increases,

Turning to the bedding materials, the PVC bedding recorded the most stable performance, with an increase of FIGRA of +79,5% and of THR of +13% BEDDING_LSA shows a FIGRA increase of only +638 W/s, reflecting a rise of +92,9% and a ΔTHR of +1.8 MJ/m² (+18,4%). This contrasts sharply with BEDDING_G which exhibits a larger increase in ΔFIGRA (+2963 W/s, +125%) and a ΔTHR (%) of +20,4% (+3.8 MJ/m²). The greater increase in both metrics suggests that the HF bedding is more susceptible to fire growth and higher heat release, when exposed to higher incident heat fluxes. Lastly, the G16 insulation exhibits a high increase in FIGRA (+4603 W/s, +99,6%), though it showed no change in THR (ΔTHR = 0 MJ/m²). This is rationalized by observing the weight loss, that was complete both at 35 kW/m² and 62 kW/m².

Similar behavior is seen in the G17 insulation, with a FIGRA percentage increase of +179,7% (+2349 W/s) and a ΔTHR (%) increase of +29,3% (+6.6 MJ/m²), reflecting the tendency of HF compounds to experience more pronounced fire growth under increased thermal stress. When comparing the S17 insulation, which is PVC-based,

to G17, the halogen-free alternative, we notice that S17 (ΔFIGRA: +2878 W/s, +112,5%; ΔTHR: +4,7 MJ/m²,+23,3%) performs more consistently at higher incident heat fluxes.

4.2.3.2 Smoke Results

The main parameters assesed by cone calorimetry to evaluate smoke emissions are pSPR, TSP and SMOGRA. pSPR and TSP are two parameters derived from the SPR curve, the first one being the maximum of the curve and the second its integral. SMOGRA is a mathematically calculated index related to smoke growth rate. For the SMOGRA to be registered by the instrument there are two requiremnets, first the TSP has to be over 6 m^2 and second the value of the SPR has to be over 0.1 m^2 for 60 continuative seconds.

The results of TSP are reported in Figure 4.15.

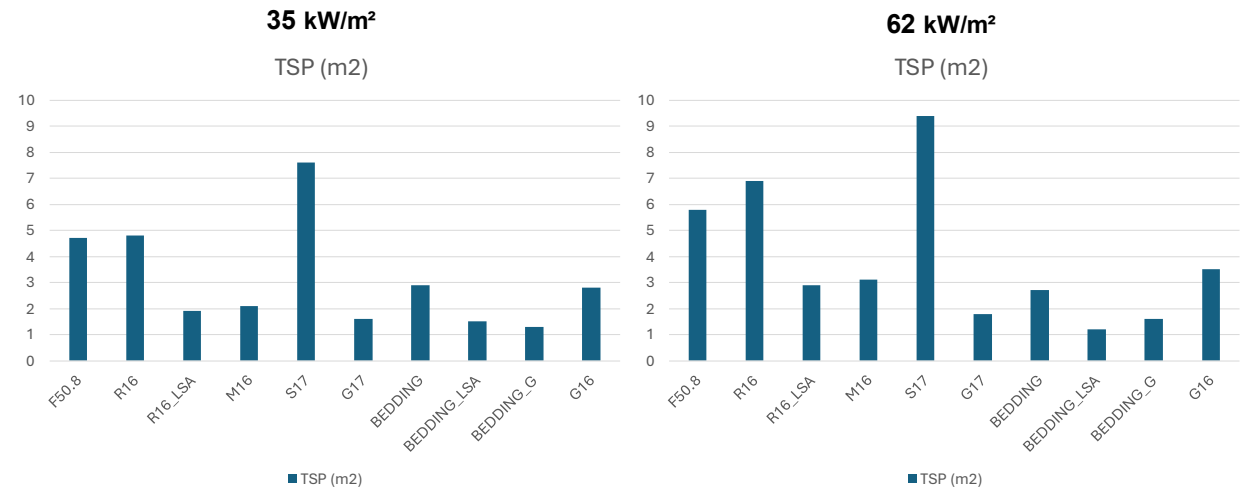

***Figure 4.15**: TSP results.*

At 35 kW/m² the TSP of R16 was 4,8 ± 0,1 m², instead the HF counterpart (M16) registered lower values (2.1± 0,0 m²). Among the LSA formulations for outer jackets, while F50.8 performs similarly to R16, R16_LSA has a much lower TSP (1,9 ± 0,2 m²). The PVC bedding recorded a TSP of 2,9 ± 0,2 m², instead, both the HF counterpart and the LSA alternative registered slightly lower values than the PVC bedding (1.3 ± 0,1 m² and 1.5 ± 0,3 m², respectively). At 62 kW/m², most of the compounds manifested a slight increase in the value of TSP, but with no significant

difference. Notably, both PVC beddings at higher incident heat fluxes registered a value slightly lower than at 35 kW/m².

These results align with the fire classifications related to smoke emissions for the corresponding cable geometries. Specifically, R16 and PVC bedding, with higher TSP values, are used in FG16OR16 cables, which fall into the s3 smoke class. In contrast, M16 and BEDDING_G recorded lower TSP values and are used in halogen-free FG16OM16 cables, classified as s1b. Finally, both R16_LSA and PVC BEDDING_LSA demonstrated very low TSP values of 2,9 ± 0,2 m² and 1,2 ± 0,3 m², respectively, that are similar to those obtained by the HF formulations. These results are coherent with the different class regarding smoke, outlined by CEI UNEL 35016 [35], achieved by the respective cable in which these compounds are used, s1b for the HF cable and s1 for FG16OR16 LSA cable developed by PVC4cables.[46] Lastly, when comparing S17 and G17 (0,023 ± 0,002 at 35 kW/m² and 0,037 ± 0,002 at 62 kW/m²), the PVC based compound shows significantly higher smoke production (0,116 ± 0 at 35 kW/m² and 0,151 ± 0,002 at 62 kW/m²) across both incident heat fluxes, consistent with the different smoke class that have to achieve FS17 (s_3) and FG17 (s_{1b}) cable geometries.

The results of pSPR are reported in Figure 4.16.

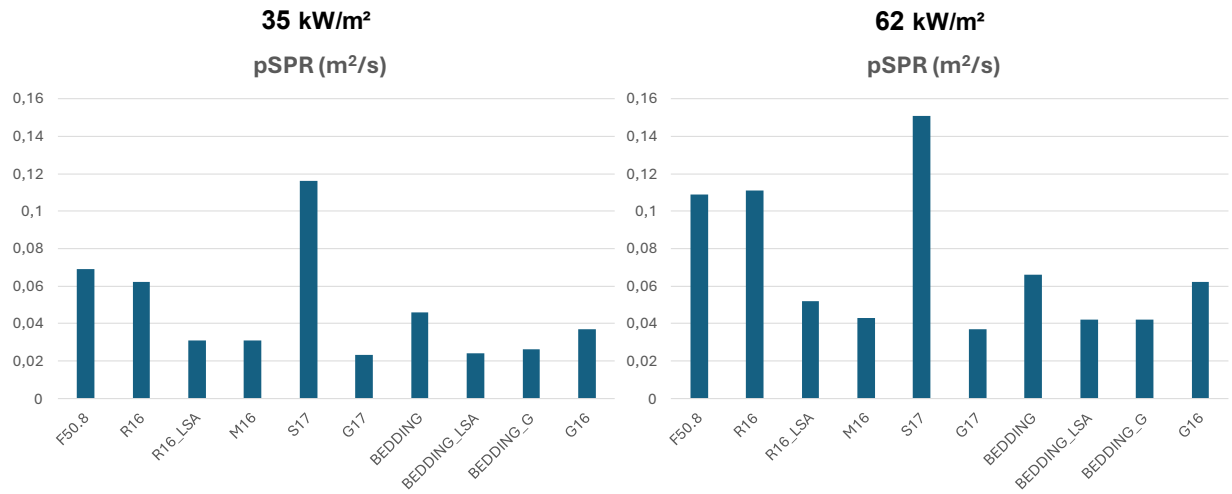

***Figure 4.16**: pSPR results.*

At 35 kW/m² the pSPR of R16 was 0,062 ± 0,002 m^2/s, similar to the peak of F50.8 and higher than the peak of R16_LSA. Also M16 showed a peak lower than R16, with values similar to R16_LSA. The PVC bedding exhibited the highest value of pSPR among beddings, while BEDDING_LSA and the HF bedding exhibited similar values. S17 displayed a much higher value than G17. At 62 kW/m², all compounds showed an increase in the value of pSPR, but with no substantial difference in trends.

The graphs reported below, in Figure 4.17 and Figure 4.18, show the SPR curves, at 35 kW/m² and 62 kW/m², of compounds used in the manifacture of cables of FG16OR16, FG16OM16, FS17 and FG17 geometries: In the top left corner are represented the SPR curves of R16, the PVC bedding and G16 (FG16OR16); in the top right corner the SPR curves of M16, the HF bedding and G16 (FG16OM16); in the bottom left corner the SPR curves of R16_LSA, BEDDING_LSA and G16 (LSA version of FG16OR16); in the bottom right corner the SPR curves of S17 and G17 (FS17 vs FG17).

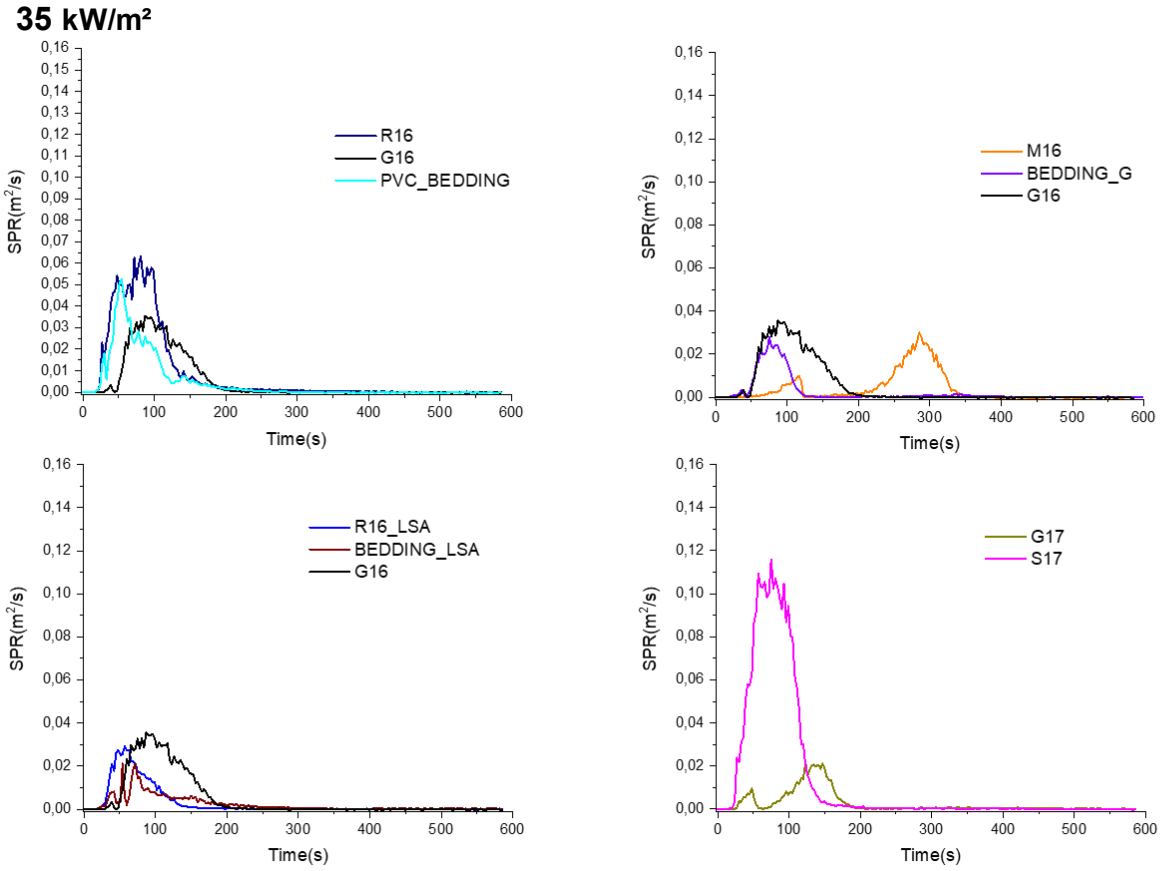

***Figure 4.17**: SPR curves at 35 kW/m² of: compounds of FG16OR16 (top left); compounds of FG16OM16 (top right); LSA alternatives for compounds of FG16OR16 (bottom left); compounds of FS17 and FG17 (bottom right).*

As expected, the SPR curves exhibites patterns mirroring the ones displayed in HRR curves, as the emission of smoke is related to the different stages of decomposition of a material.

At 35 kW/m², R16 exhibited a broad peak around 100 seconds (pSPR of 0,062 ± 0,002 m²/s), while M16 showed a very small initial peak around 100 seconds, followed by a delayed second peak at approximately 300 seconds with a pSPR of 0,031 ± 0,001 m²/s. Compared to R16, R16_LSA displayed a narrower and lower peak (0,031 ± 0,004 m²/s) at around 70 seconds, while, it displayed the same value of pSPR registered by M16. The PVC bedding showed a peak around 70 seconds with a pSPR of 0,046 ± 0,009 m²/s, significantly higher than that of BEDDING_G, which registered a pSPR of 0,026 ± 0,002 m²/s at similar times. The LSA PVC bedding formulation displayed two narrow and low peaks (pSPR of 0,024 ± 0,004 m²/s) before 100 seconds. For the insulation materials, G16, used as inner insulation common to both FG16OR16 and FG16OM16 cables, exhibited a very broad curve ranging from 50 seconds to 200 seconds. Lastly, S17 recorded a much higher peak (pSPR of 0,112 ± 0,000 m²/s) compared to G17 (pSPR of 0,023 ± 0,002 m²/s), with

S17 slightly shifted to earlier times.

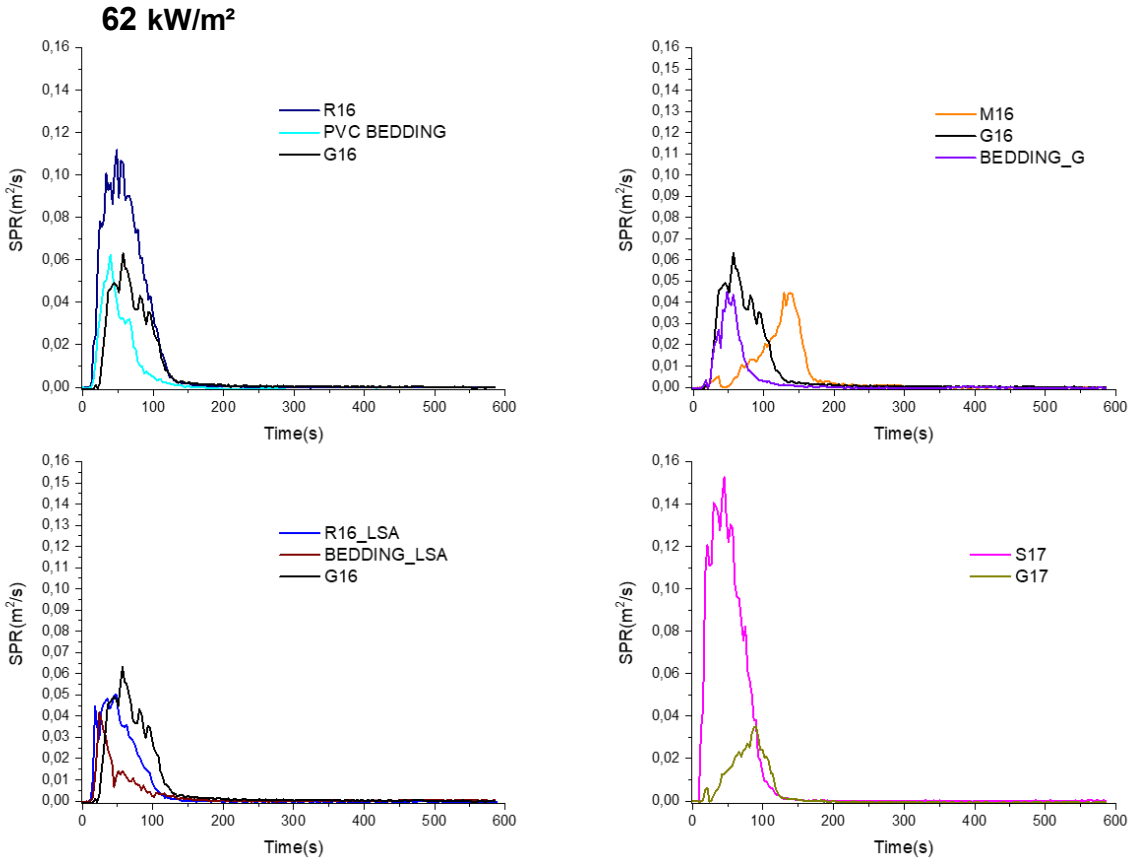

***Figure 4.18**: SPR curves at 62 kW/m² of: compounds of FG16OR16 (top left); compounds of FG16OM16 (top right); LSA alternatives for compounds of FG16OR16 (bottom left); compounds of FS17 and FG17 (bottom right).*

At 62 kW/m², R16 exhibited a narrower peak at earlier times, with a higher pSPR of 0,111 ± 0,001 m²/s, compared to the curve observed at 35 kW/m². M16 displayed similar behavior, with a slight increase in peak intensity and a significant shift to earlier times, around 150 seconds, compared to the lower incident heat flux. R16_LSA showed a peak occurring before 100 seconds, with a pSPR increased to 0,052 ± 0,005 m²/s, if compared to the the peak obtained at lower heat fluxes. For the bedding materials, the PVC bedding showed almost no increase in peak intensity, with only a slight shift to earlier times compared to the 35 kW/m² curve. In contrast, the HF bedding registered an increase in pSPR to 0,042 ± 0,004 m²/s, while the LSA bedding also increased to 0,042 ± 0,005 m²/s. Lastly, at the higher incident flux, the time gap in smoke emissions between S17 and G17 narrowed, providing that the

pSPR of G17 shifted at earlier times, though the substantial difference in intensity remained.

4.2.4 Discussion of results' trends

From LOI measurements the main trends observed were:

- F50.8 and R16_LSA showed decreased LOI compared to R16, this is due to the acid scavenger's role in trapping the HCl released from the decomposition of the PVC resin, preventing the inherent mechanism of flame poisoning of PVC.
- M16 showed higher LOI than R16, reflecting its role as primary defence to fire in FG16OM16 cables.
- PVC based beddings manifested higher LOI than HF based ones.
- S17 and G17 exhibited similar results.
- G16 showed the worst results among all compounds.

From MCC measurements the main trends observed were:

- F50.8 showed similar flammability in respect to R16, across all parameters evaluated.
- R16_LSA manifested lower flammability compared to R16, across all parameters evaluated.
- M16 exhibited worst results, in terms of flammability, in respect to R16 across all parameters evaluated.
- While the LSA alternative for bedding showed slightly lower flammability than the standard PVC bedding, the HF registered substantially higher results, regarding flammability, across all parameters evaluated.
- G16 recorded the worst results among all compounds.

From Cone Calorimetry measurements the main trends observed were:

- PVC based compounds registered lower TTP in respect to the corresponding HF alternatives, showing a narrowed gap at higher incident heat fluxes.
- HF compounds showed higher THR, in respect to PVC based compounds.

- While M16 exhibited a lower FIGRA than R16, the HF bedding result for FIGRA was much higher than for the PVC bedding.
- HF compounds suffered a greater decrease in reaction-to-fire in response to higher incident heat fluxes, if compared to PVC based compounds.
- R16_LSA had similar FIGRA and THR to R16, across both heat fluxes.
- BEDDING_LSA showed better reaction-to-fire than regular PVC bedding, particularly at higher heat fluxes.
- The TSP of both LSA and HF formulations, were much lower than for standard PVC based compounds.

These three analytic techniques cannot be directly compared to each other. In fact, LOI, MCC and Cone measurements were conducted under different settings, regarding temperatures, oxygen concentrations and times. In particular, MCC and Cone Calorimetry are conducted under a heat ramp and isotherm conditions, respectively. Thus, values containing slopes, temperatures, times and index mathematically calculated on this basis cannot be compared.

The only values that can be compared, not in absolute value because of different kinetics taking place at different settings, but only as a trend among different compounds, is the specific total heat released from MCC (h_c) and Cone Calorimetry analysis (THR).

The specific total heat released from Cone Calorimetry was calculated by dividing the THR (MJ/m^2) by the initial weight of the sample (expressed in g) and by multiplying for the irradiated area of the sample (in m^2). Table 4.19 presents the specific total heat released from Cone Calorimetry and MCC.

Compound	**THR (J/g) *(35 kW/m²)***	**THR (J/g) *(62 kW/m²)***	***h_c* (J/g)**
R16	9200	12100	12,26
F50.8	10200	11200	13,51
R16_LSA	7600	8500	8,65
M16	12900	15100	16,59

PVC BEDDING	5600	6600	6,29
PVC BEDDING_LSA	3800	4900	5,36
BEDDING_G	8600	9900	10,27
G16	42900	44500	49,75
S17	11300	12700	13,70
G17	12100	15200	18,67

***Table 4.19**: Specific THR values from Cone Calorimetry (at both heat fluxes) and MCC (h_c).*

The trends of the Specific total heat released from Cone and MCC were coherent:

- PVC based compounds exhibited lower values than the corresponding HF alternatives.
- The LSA formulations for outer jacket and bedding, developed by PVC4cables, recorded lower values than standard PVC compounds.
- G16 registered the highest value.

5. CONCLUSIONS

The harmonized regulatory framework within the European Union, specifically CPR Regulation (EU) No 305/2011, includes fire safety among the basic seven requirements for construction products, including cables permanently installed in buildings. EN 50575 and EN 13501-6 provide the basis for testing, classification, and certification of cables in relation to their fire behavior. In Italy, CEI UNEL 35016 further defines the classification system based on specific fire risk assessments. In this study, various cable compounds, ranging from PVC based materials commonly found in the market, like R16, S17, and PVC beddings, to LSA PVC formulations and HF alternatives, were tested to assess their fire performance by LOI, MCC and Cone measurements. The compounds tested are used in the production of various cable geometries, such as FG16OR16 and FS17, along with their halogen-free counterparts, FG16OM16 and FG17.

Regarding FS17 and FG17, S17 MCC parameters are all better than G17 ones. Furthermore, S17 compounds showed a better THR and a worse FIGRA, driven by the higher TTP than G17. Unfortunately, at both incidental heat fluxes, the TSP from S17 is about 5 times higher than G17. It needs to be highlighted that S17 is a standard grade PVC compounds and further research should be done for developing new LSA compounds for insulation.

Regarding FG16OR16 and FG16OM16 cables, G16 displayed poor reaction-to-fire, emphasizing its role as inner insulation. Findings highlighted the different strategies adopted in commercially available cable geometries to shield the less fire performant G16. In FG16OR16 cables, it is exploited the ability of PVC-based beddings in enhancing the reaction-to-fire of the cable system, particularly in comparison to their halogen-free counterparts. In fact, not only it reduces the heat release, and the flame spread, but also prevents the flaming dripping of non-flame retarded G16, preventing it from sliding over the bedding (due to its incompatibility) and generating flaming droplets. Instead, in FG16OM16 the focus is on the outer jacket of M16 quality, presenting good reaction-to-fire, and less on the bedding (no problems of

compatibility with G16). Confronting results from Cone tests, the only advantages that are provided by HF are the higher TTIs and TTPs which affect the the ignition point and the time at which the peak of HRR curve reaches the maximum. M16 registered a lower FIGRA than R16. Though, these gaps are substantailly narrowed when irradiating the sample with higher incident heat fluxes. Once the HF reached a higher incident heat fluxes it release much more heat than the PVC counterparts. THR results trends, higher values for HF compounds, were coherent with the results of specific total heat released obtained with MCC. HF counterparts displayed higher flammability than standard PVC based compounds, across all parameters assessed by MCC.

The smoke results obtained from the compounds used to manifacture FG16OR16 LSA were much better than the respective standard PVC compounds, their performances were similar to the ones obtained from the correspondent HF compound. It's a well-known fact that PVC based compounds tend to emit more smoke than HF compounds, but the results from Cone measurements proved that, with effective additivation, PVC based compounds can compete in terms of smoke emissions with HF counterparts. Furthermore, LSA formulations displayed better performance to fire than standard PVC compounds, and particularly, lower THR than HF alternatives.

6.MATERIALS AND METHODS

6.1 DRY BLENDS AND SAMPLES PREPARATION

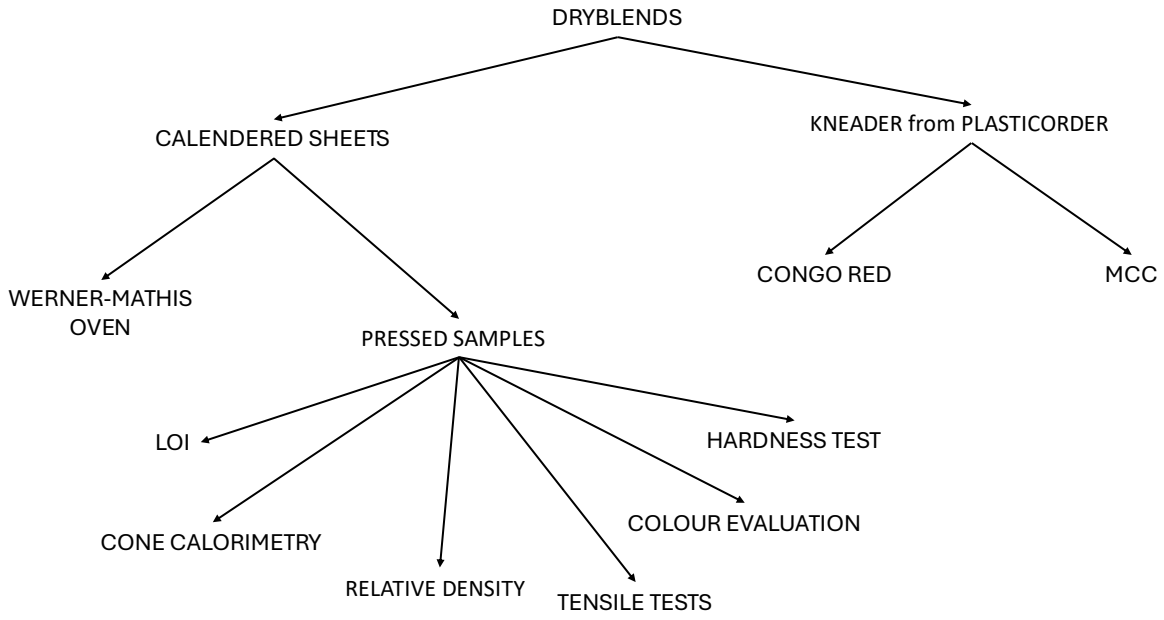

***Figure 6.1**: chart of the sample preparation.*

6.1.1 Preparation of dryblends

The dry blends were prepared as described in this section using a lab-scale turbo mixer device from Henschel (a picture is reported in Figure 6.2). To ensure no cross-contamination from previous batches, a cleaning cycle was conducted before starting each new formulation. The PVC resin along with all solid components were placed into the mixer. 3500 g were used for each blending. Mixing of powder was commenced at about 1300 rpm and kept for two minutes. Then, about a third of the liquid ingredients, previously mixed, were gradually introduced to moisten the powders for more effective blending. Once the temperature of the mixing blend reached 60 °C, the rest of the liquid phase was added in stages: each time the temperature increased by 5 °C, a small amount was introduced to keep the mixture moist until the temperature reached 90 °C, at which point the final addition was

made. The process was halted when the mixture reached 105 °C, and the batch was then collected in a clean bag.

***Figure 6.2**: lab-scale turbo mixer device form Henschel*

6.1.2 Calendering

It was used the MCC/N150X300-E model by Battaggion. About 180 g of each dry blend was fed into the calendering machine. The distance between the rollers was set at 0.30 mm, the temperature was set at 160 °C and each process was stopped after 3 minutes.

6.1.3 Pressing

Following the production of PVC sheets via the calendering process, these sheets were further processed using a heated press to produce pressed samples of different thickness and dimensions depending on the kind of test specimen to be prepared.

The press's temperature was controlled at 160°C, with suitable amount of material allocated in the mold for each pressing cycle, and the duration set to 4 minutes. The applied pressure underwent a timed escalation: starting at 20 bar, it was increased to 50 bars after the initial 1 minute and 30 seconds. Subsequently, the pressure was increased to 100 bars following another 1 minute and 30 seconds interval, before being gradually elevated to 150 bars during the cooling phase's first minute. Once the pressing process concluded and the press returned to room temperature, the final specimen was retrieved.

6.2 SAMPLE CHARACTERIZATION

6.2.1 Hardness Test

The hardness of elastomers and rubber polymers is assessed using the testing procedures specified in ISO 7619-1 and ASTM D2240 technical standards. The Shore A hardness test utilizes a truncated cone indenter with a 35° angular opening. This method measures the depth of penetration of a spring-loaded indenter into the material, with different depths indicating varying hardness levels. Specifically, a shallower indentation signifies a harder material. The measurement is recorded after 15 seconds.

The test was performed on specimens consisting into pressed material 4x4 cm squares with a thickness of 6 mm. A manual digital hardness tester (Gibitre Instrument), shown in Figure 6.3, was used for this evaluation. The test was repeated 12 times for each specimen and the resulting average and standard deviation were obtained.

***Figure 6.3**: manual digital hardness tester from Gibitre Instrument*

6.2.2 Tensile Test

The tensile test, also known as the uniaxial tensile test, is a materials characterization method that involves applying an initially zero uniaxial load F to a standard-sized specimen. This load is progressively increased to a maximum value until the material ultimately fails.

The tensile test is used to determine various properties of the material being tested, such as Young's modulus (E, defined as the ratio between stress and strain), the load at failure, and the percent elongation at failure. The instrument used for this test is Z005 Zwick/Roell dynamometer, as depicted in Figure 6.4. The test follows the ISO 527-1 standard, using specimen type 1A.

***Figure 6.4**: Z005 Zwick/Roell dynamometer*

The test was also performed on specimen after a period of aging of 10 days at 100 °C, as described by the CEI EN 50363-0. [44]

The experiments were repeated 5 times for each specimen and the averages along with their standard deviations were estimated

6.2.3 Rheology

The plasticorder is an instrument designed to measure the torque (viscosity) of plastic materials as they respond to changes in time and temperature. In accordance with ASTM D 2538, a predetermined quantity of dryblend is placed into the thermostated chamber of the instrument via a quick-loading chute. A ram is then inserted into the chute, and a weight is applied. Within the 50 cm^3 chamber, the compound is exposed to heat and shear stress generated by two internal roller-style blades rotating at a specified rate. The conditions set for the analysis were 160 °C, 20 rpm and 10 minutes for 64 g of specimen. The plasticorder used is depicted in Figure 6.5.

***Figure 6.5**: plasticorder device from Brabender*

6.2.4 Colour evaluation

To evaluate the initial colour of plastic materials, a colorimetric analysis was conducted using the X-Rite QA2000 colorimeter. This instrument allows for the precise numerical identification of colour within the CIE colour space (a representation is reported in Figure 6.6), represented by three values: L*, a*, and b*. The L* value denotes the brightness level, expressed as a percentage, where 0 corresponds to black and 100 to white. The a* value indicates the colour direction on the green-red axis, with negative values signifying green and positive values signifying red. Similarly, the b* value represents the colour direction on the blue-yellow axis, with negative values indicating blue and positive values indicating yellow.

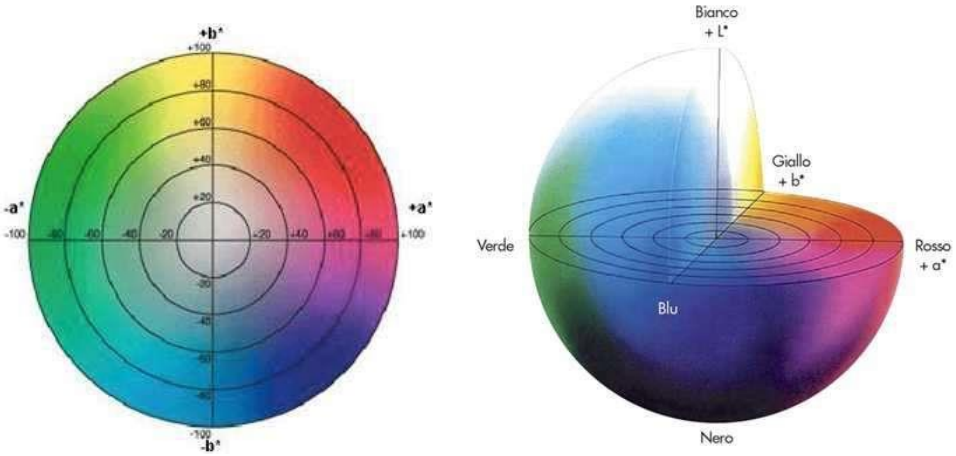

***Figure 6.6**: Graphical representation of the colour space*

6.2.5 Relative Density

Relative density can be measured through multiple techniques. For solid objects with a density higher than water, the process involves first weighing the object in air, followed by weighing it while fully submerged in water. According to Archimedes' principle, the relative density is then determined by dividing the weight in air by the difference in weight when the object is immersed. The instrument used to evaluate densities is presented in Figure 6.7.

***Figure 6.7**: instrument used to evaluate relative density*

Three measurements were taken for each sample: three in air and three fully submerged in water

6.3.6 Thermal stability

The thermal stability of PVC compounds is assessed using the EN 60811-405 technical standard, commonly known as the Congo Red Test, which is widely used in the electrical cable industry. This test measures the time taken for Congo red paper to change color due to HCl emission. The instrument used for this test is a Liebisch block thermostat, model Liebisch Labortechnik LT-PVC-210-36-5, shown in Figure 6.8.

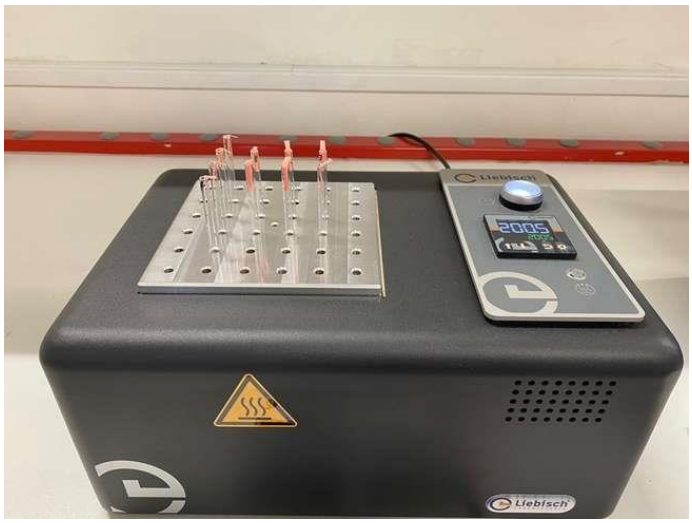

***Figure 6.8**: Liebisch Labortechnik LT-PVC-210-36-5*

A sample weighing 50 ± 5 mg is placed in a glass tube and inserted into the block thermostat set at 200 ± 0.5 °C. A piece of Congo red paper is positioned at the top of the tube, the colour changing from pink to blue when the PVC starts emitting HCl. The Congo red value represents the time interval from the beginning of the test to the moment the Congo red paper turns blue.

Specimens were prepared from calendered sheets and evaluated both before and after aging.

6.3.7 Wener-Mathis Oven

Using a Werner Mathis Oven, we can assess colour retention over time, and long-term thermal stability. To perform this evaluation, test specimens were prepared using a pleating machine on calendered sheets, which are placed in the oven and maintained at a temperature of 200°C. Throughout the process, the specimens are moved outward at a rate of 0.5 cm every 120 seconds. The instrument used for this procedure is reported in Figure 6.9.

***Figure 6.9**: Thermotester used to assess colour retention over time*

6.3 HIGH TEMPERATURE AND FIRE BEHAVIOUR TESTS

6.3.1 LOI

The Limiting Oxygen Index, as outlined in the ASTM D 2863 technical standard, indicates the lowest concentration of oxygen (expressed as a percentage volume in an oxygen-nitrogen mixture) needed to sustain the combustion of a material at a starting temperature of 23°C ± 2°C. To measure the LOI, the ASTM D 2863 procedure is followed using an FTT (Fire Testing Technology) device (Figure 6.10).

***Figure 6.10**: equipment used to obtain LOI values.*

A test specimen, having specified dimensions selected among the ones defined by ASTM D 2863 (10.5 cm of length, 6.2 cm of width and 3 mm of thickness, refer to Figure 6.11), is positioned vertically in a glass column with a controlled flow of an oxygen/nitrogen mixture. The top of the specimen is ignited, and the combustion behaviour is monitored, noting the duration and extent of burning. By testing multiple specimens at varying oxygen levels, the LOI, the minimum oxygen concentration required to keep the material burning, is determined.

***Figure 6.11**: specimen of dimensions defined by ASTM D 2863*

6.3.2 MCC

Microscale Combustion Calorimetry is a technique used to assess a material combustion and decomposition pattern on a microscale level, evaluating parameters

such as the maximum specific heat release, the heat release capacity and the fire growth capacity.

The analyses were performed in accordance with the Method A provided by ASTM D 7309 standard, with the instrument shown in Figure 6.12, Standard Model from FTT.

***Figure 6.12**: MCC*

ASTM 7309 testing was conducted on three replicates following method A, with the mean and standard deviation calculated. The instrument is divided into two sections, the pyrolizer and the combustor. Nitrogen was flowed at 80 mL/min in the pyrolizer and oxygen at 20 mL/min in a mixing chamber along to the gas and vapours coming from the pyrolizer. The combustor temperature was maintained at 750 ± 1°C, while the pyrolizer was heated at a rate of 1°C/min up to 750°C. The sample was placed in a ceramic pan and the weight (from 2 to 35 mg) was recorded. The ceramic pan was

then placed on a sample holder which was finally loaded into the pyrolizer to start the test. As samples are heated, the volatile gases are purged from the pyrolysis zone and mixed with oxygen to provide a comburent, and then flowed into the combustor. At the outlet of the combustor there is a sensor recording the O_2% flowing, the heat release rate is determined by measuring the oxygen drop. Oxygen consumption was monitored to ensure it remained within a drop range of starting O_2%-13% and starting O_2%-7% during the trial. Key combustion properties obtained from the experiment include yield of pyrolysis residue (Y_p), specific (total) heat release (h_c), maximum specific heat release rate (Q_{max}) and heat release capacity (η_c). Another parameter derived from the analysis is the Fire Growth Capacity (FGC), calculated as reported in eq. (1).

$$FGC = \left[\frac{hc}{T_{95\%} - T_{5\%}}\right]\left[\frac{T_{95\%} - T_0}{T_{5\%} - T_0}\right] \quad (1)$$

where h_c is the total Heat Release of the specimen during the test (J/g), T_0 (K) is the standard room temperature, T_0 = 298K , $T_{5\%}$ (K) is the Ignition Temperature, which is approximated by the temperature at which 5% of Q∞ has been released, and $T_{95\%}$ (K) is the temperature at which 95% of Q∞ has been released, which approximates the surface burning temperature.

6.3.3 Cone Calorimetry

In a standard cone calorimeter test, a sample is placed on a load cell (model presented in Figure 6.13), while a cone-shaped radiant heater above it delivers a uniform heat flux.

***Figure 6.13**: specimen placed on a load cell after the analysis.*

Before the test begins, the sample is shielded from the heat by a shutter mechanism. Once the shutters are opened and the experiment starts, the gases released by the sample are ignited by an electric spark. The gases produced during combustion are drawn into an exhaust duct by a fan and hood system, with a portion of these gases captured by a sampling unit for analysis. Key measurements taken during the test include gas flow, concentrations of oxygen, smoke density, and mass loss. By evaluating the rate of oxygen consumption resulting from combustion, the rate of heat release can be quantified [34]. Additional parameters such as time Time To Ignition (TTI), Time to Flame Out (TFO), Time To Peak (TTP), Total Smole Production (TSP), Smoke Production Rate (SPR), peak Smoke Production Rate (pSPR) are evaluated. The load cell weight is first recorded by the instrument using a scale that allows the tracking of the sample weight, so to evaluate the Weight Loss. FIGRA is calculated according to equation (2) given by EN 50399:2016.

$$FIGRA = 1000 \times Max\left[\frac{HRRav}{t - t_i}\right] \qquad (2)$$

where HRRav is 30 second average value of Heat Release Rate (kW/m^2), t is time after ignition (s) and t_i is ignition time (s).

It was used a cone calorimeter from FTT, designed and constructed following ISO 5660/ASTM E 1354. All measurements were performed in accordance with ISO 5660. The experimental set-up is shown in Figure 6.14.

***Figure 6.14**: cone calorimetry set-up*

The specimens (100 x 100 x 2,50 mm) were prepared using a heated press, a model is presented in Figure 6.15.

***Figure 6.15**: model of samples used for cone calorimetry measurements.*

The experiment was conducted using two specific heat fluxes: at 35 kW/m² and 62 kW/m², the average and standard deviations of the results were obtained.

BIBLIOGRAPHY

[1] Regulation (EU) No 305/2011 of the European parliament and of the council of 9 March 2011 laying down harmonized conditions for the marketing of construction products and repealing Council Directive 89/106/EEC. Consolidated version 16/07/2021.
https://eur-lex.europa.eu/legal-content/EN/TXT/?uri=CELEX%3A02011R0305-20210716.

[2] EN 50575. Power, control and communication cables. Cables for general applications in construction works subject to reaction to fire requirements. Current version EN 50575:2014+A1:2016.

[3] EN 13501-6. Fire classification of construction products and building elements - Classification using data from reaction to fire tests on power, control and communication cables. Current version EN 13501-6:2019.

[4] Plastic Europe (2023), Plastic - The fast facts 2023.
https://plasticseurope.org/knowledge-hub/plastics-the-fast-facts-2023/

[5] Plastic Europe. (2020). Plastics- the fact 2020: an analysis of European plastics production, demand and waste data".
https://plasticseurope.org/

[6] EN 60754-1 Test on gases evolved during combustion of materials from cables - Part 1: - Part 1: Determination of the halogen acid gas content.
Current version. EN 60754-1:2014/A1:2020.

[7] J.J Beitel, C.A Bertelo, W.F. Carrol Jr, R.O. Gardner, A.F.Grand, M.M. Hirschler, G.F.Smith. Hydrogen chloride transport and decay in a large apparatus I. decomposition of PVC wire insulation in a plenum by current overload: Journal of fire sciences, 1986, 4(1), 15-41. https://doi.org/10.1177/073490418600400103.

[8] T.R. Hull, A.A. Stec, K.T. Paul. Hydrogen Chloride in Fires, Proceedings of the 8th International Symposium on Fire Safety Science, 2008. https://www.iafss.org/publications/fss/9/665/view/fss_9-665.pdf.

[9] M. Hirschler. Fire safety, smoke toxicity and acidity: Flame Retardants 2006, February 14-15, 2006, London, Interscience Communications, London, UK (2006), Pages 47-58. https://gbhint.tripod.com/papers_5_13_02/246_Toxfr94.pdf.

[10] M. Hirschler. Fire Performance of Organic Polymers, Thermal Decomposition, and Chemical Composition. Chapter 23 in "Fire and Polymers", 2001, 293-306. https://doi.org/10.1021/bk-2001-0797.ch023.

[11] V. Babrauskas, R. D. Peakock. Heat release rate: The single most important variable in fire hazard, Fire Safety Journal, 1992, 18(3), 255 – 272. https://doi.org/10.1016/0379-7112(92)90019-9.

[12] E.Weil, S,Levchik. Flame and Smoke Retardants in Vinyl Chloride Polymers – Commercial Usage and Current Developments: Journal of fire, 2006, 24(3), 211-236. https://doi.org/10.1177/0734904106057951

[13] C. E. Wilkes, J. W. Summers, C. A. Daniels, Mark T. Berard. (2005). "PVC Handbook". (1st ed.). Hanser.

[14] The European Council of Vinyl Manufacturers. https://pvc.org/about-pvc/vinyl-chloride-monomer-vcm-production/#:~:text=There%20are%20two%20methods%20to,a%20few%20hundred%20degrees%20Celsius.

[15] R. Bacaloglu, M. Fish. Degradation and stabilization of Poly(viny1 chloride). V. Reaction mechanism of Poly(viny1 chloride) degradation: Polymer Degradation and Stability, 1995, 47 (1), 33-57. https://doi.org/10.1016/0141-3910(94)00086-N.

[16] W.H. Starnes Jr. Structural and mechanistic aspects of the thermal degradation of poly(vinyl chloride): Progress in Polymer Science, 2002, 27(10), 2133-2170. https://doi.org/10.1016/S0079-6700(02)00063-1.

[17] W. H. Starnes, Jr., J. A. Wallach, and H. Yao, 1996, "Six-Center Concerted Mechanism for Poly(vinyl chloride) Dehydrochlorination. Requiescat in Pace? 1996, 29(23), 7631−7633. https://doi.org/10.1016/0141-3910(94)00086-n.

[18] W.H. Starnes, Jr., X. Ge. Mechanism of Autocatalysis in the Thermal Dehydrochlorination of Poly(vinyl chloride): Macromolecules, 2004, 37(2), 352–359. https://doi.org/10.1021/ma0352835.

[19] Directive 2002/95/EC of the European Parliament and of the Council of 27 January 2003 on the restriction of the use of certain hazardous substances in electrical and electronic equipment. https://eur-lex.europa.eu/legal-content/EN/TXT/?uri=CELEX%3A02002L0095-20110910.

[20] VINYL 2010, "The Voluntary Commitment of the PVC Industry", Vinylplus. https://vinylplus.eu/uploads/Modules/Documents/vc2001_en.pdf.

[21] ISO 13943:2017, "Fire Safety – Vocabulary", ISO, https://www.iso.org/standard/63321.html.

[22] ASTM D 7309

[23] EN 50399. Common test methods for cables under fire conditions. Heat release and smoke production measurement on cables during flame spread test. Test apparatus, procedures, result. https://doi.org/10.3403/30095951U.

[24] ASTM E 662. Standard method test for specific optical density of smoke generated by solid materials.

[25] M.Werrel, J.H. Deubel, S.Kruger, A.Hofmann, U.Krause. The calculation of the heat release rate by oxygen consumption in a controlled atmosphere cone calorimeter: Fire and Materials, 2014, 38(2), 204-226. https://doi.org/10.1002/fam.2175.

[26] F. Laoutid, et al. New prospects in flame retardant polymer materials: from fundamentals to nanocomposites: Material Science and Engineering Reports, 2009, 63(3), 100-125. https://doi.org/10.1016/j.mser.2008.09.002.

[27] C.H. Wu, C.Y Chang, J.L Hor. Two stage pyrolysis model of PVC: PVC. Can J Chem Eng, 1984 72(4): 644–650. https://doi.org/10.1002/cjce.5450720414.

[28] EN 60754-1 Test on gases evolved during combustion of materials from cables - Part 1: - Part 1: Determination of the halogen acid gas content. Current version. EN 60754-1:2014/A1:2020.

[29] EN 60754-2 Test on gases evolved during combustion of materials from cables - Part 2: Determination of acidity (by pH measurement) and conductivity. Current version. EN 60754-2:2014/A1:2020.

[30] "CPR-PVC cables document". PVC4Cables. (2018). https://www.pvc4cables.org/

[31] Astrid Aupetit (2021). Overview of the Global Cable Industry – Market and Materials. In G. Beyer (Eds). The Global Cable Industry. (Chapter 1). Wiley.

[32] Official Journal of the European Union, "COMMISSION DECISION of 27 October 2006 amending Decision 2000/147/EC implementing Council Directive 89/106/EEC as regards the classification of the reaction-to-fire performance of construction products"

[33] The European Council of Vinyl Manufacturers. https://pvc.org/about-pvc/vinyl-chloride-monomer-vcm-production/#:~:text=There%20are%20two%20methods%20to,a%20few%20hundred%20degrees%20Celsius.

[34] W. H. Starnes et al. (1982). Mechanism od Poly(vinyl chloride) fire by molybdenum (VI) Oxide. Further evidence in favor of the Lewis acid theory. In E. Kresta (Eds). Polymer additives. Volume 26, (pp 237 – 248).

[35] CEI-UNEL 35016 Class of reactions to fire of the cables in relation to the EU "Construction Products Regulations" (305/2011).

[36] Payne, Lynda B., "The Dehydrochlorination Mechanism of the Internal Allylic Chloride Structure in Poly(Vinyl Chloride)" (2000). Dissertations, Theses, and Masters Projects. William & Mary. Paper 1539626253. https://dx.doi.org/doi:10.21220/s2-x2cs-0908.

[37] Kaplan, H.L, Grand, A.F., Switzer, W.G., Mitchell, D.S., Rogers, W.R. and Hartzell, G.E.,"Effects of Combustion Gases on Escape Performance of the Baboon and the Rat", J. Fire Sciences, 3, 228-244 (1985).

[38] Reporter's Guide: All about fire. (n.d.). https://www.nfpa.org/about-nfpa/press-room/reporters-guide-to-fire/all-about-fire

[39] Bassi, I.; Delchiaro, F.; Bandinelli, C.; Mazzocchetti, L.; Salatelli, E.; Sarti, G. A New Perspective on Hydrogen Chloride Scavenging at High Temperatures for Reducing the Smoke Acidity of PVC Cables in Fires, IV: The Impact of Acid Scavengers at High Temperatures on Flame Retardance and Smoke Emission. Fire 2023, 6, 259. https://doi.org/10.3390/fire6070259,

[40] ISO 472:2013 – Plastics – Vocabulary

[41] Aasberg-Petersen, K., Christensen, T. S., Dybkjaer, I., Sehested, J., Østberg, M., Coertzen, R. M., … Steynberg, A. P. (2004). Synthesis gas production for FT synthesis. Studies in Surface Science and Catalysis, 258–405. doi:10.1016/s0167-2991(04)80461-0

[42] Delchiaro, Francesca & Bandinelli, Claudia & Bassi, Iacopo & Piana, Marco & Sarti, Gianluca. (2024). New Generation PVC compounds for cables and safety in case of fire.

[43] Bassi, I. Characterization of PVC compounds and evaluation of their fire behavior focusing on the comparison between EN 60754-1 and EN 60754-2 in the assessment of the smoke acidity. Master thesis. University of Bologna.

[44] Xu, Q., Mensah, R. A., Jin, C., & Jiang, L. (2021). A critical review of the methods and applications of microscale combustion calorimetry for material flammability assessment. Journal of Thermal Analysis and Calorimetry. doi:10.1007/s10973-021-10963-4

[45] CEI EN 50363-0 national annex. Insulating, sheathing, and coating materials for low-voltage power cables

[46] PVC4cables, unpublished report, 2024.

[47] Reagens spa, unpublished report, 2023.

[48] open access data: https://www.baldassaricavi.it/distribution/cavi-nazionali/